

MIT OpenCourseWare  
<http://ocw.mit.edu>

Haus, Hermann A., and James R. Melcher. *Electromagnetic Fields and Energy*. Englewood Cliffs, NJ: Prentice-Hall, 1989. ISBN: 9780132490207.

Please use the following citation format:

Haus, Hermann A., and James R. Melcher, *Electromagnetic Fields and Energy*. (Massachusetts Institute of Technology: MIT OpenCourseWare). <http://ocw.mit.edu> (accessed [Date]). License: Creative Commons Attribution-NonCommercial-Share Alike.

Also available from Prentice-Hall: Englewood Cliffs, NJ, 1989. ISBN: 9780132490207.

Note: Please use the actual date you accessed this material in your citation.

For more information about citing these materials or our Terms of Use, visit:  
<http://ocw.mit.edu/terms>

# 5

## *ELECTROQUASISTATIC FIELDS FROM THE BOUNDARY VALUE POINT OF VIEW*

### 5.0 INTRODUCTION

The electroquasistatic laws were discussed in Chap. 4. The electric field intensity  $\mathbf{E}$  is irrotational and represented by the negative gradient of the electric potential.

$$\mathbf{E} = -\nabla\Phi \quad (1)$$

Gauss' law is then satisfied if the electric potential  $\Phi$  is related to the charge density  $\rho$  by Poisson's equation

$$\nabla^2\Phi = -\frac{\rho}{\epsilon_0} \quad (2)$$

In charge-free regions of space,  $\Phi$  obeys Laplace's equation, (2), with  $\rho = 0$ .

The last part of Chap. 4 was devoted to an "opportunistic" approach to finding boundary value solutions. An exception was the numerical scheme described in Sec. 4.8 that led to the solution of a boundary value problem using the source-superposition approach. In this chapter, a more direct attack is made on solving boundary value problems without necessarily resorting to numerical methods. It is one that will be used extensively not only as effects of polarization and conduction are added to the EQS laws, but in dealing with MQS systems as well.

Once again, there is an analogy useful for those familiar with the description of linear circuit dynamics in terms of ordinary differential equations. With time as the independent variable, the response to a drive that is turned on when  $t = 0$  can be determined in two ways. The first represents the response as a superposition of impulse responses. The resulting convolution integral represents the response for all time, before and after  $t = 0$  and even when  $t = 0$ . This is the analogue of the point of view taken in the first part of Chap. 4.

The second approach represents the history of the dynamics prior to when  $t = 0$  in terms of initial conditions. With the understanding that interest is confined to times subsequent to  $t = 0$ , the response is then divided into "particular"

and “homogeneous” parts. The particular solution to the differential equation representing the circuit is not unique, but insures that at each instant in the temporal range of interest, the differential equation is satisfied. This particular solution need not satisfy the initial conditions. In this chapter, the “drive” is the charge density, and the particular potential response guarantees that Poisson’s equation, (2), is satisfied everywhere in the spatial region of interest.

In the circuit analogue, the homogeneous solution is used to satisfy the initial conditions. In the field problem, the homogeneous solution is used to satisfy boundary conditions. In a circuit, the homogeneous solution can be thought of as the response to drives that occurred prior to when  $t = 0$  (outside the temporal range of interest). In the determination of the potential distribution, the homogeneous response is one predicted by Laplace’s equation, (2), with  $\rho = 0$ , and can be regarded either as caused by fictitious charges residing outside the region of interest or as caused by the surface charges induced on the boundaries.

The development of these ideas in Secs. 5.1–5.3 is self-contained and does not depend on a familiarity with circuit theory. However, for those familiar with the solution of ordinary differential equations, it is satisfying to see that the approaches used here for dealing with partial differential equations are a natural extension of those used for ordinary differential equations.

Although it can often be found more simply by other methods, a particular solution always follows from the superposition integral. The main thrust of this chapter is therefore toward a determination of homogeneous solutions, of finding solutions to Laplace’s equation. Many practical configurations have boundaries that are described by setting one of the coordinate variables in a three-dimensional coordinate system equal to a constant. For example, a box having rectangular cross-sections has walls described by setting one Cartesian coordinate equal to a constant to describe the boundary. Similarly, the boundaries of a circular cylinder are naturally described in cylindrical coordinates. So it is that there is great interest in having solutions to Laplace’s equation that naturally “fit” these configurations. With many examples interwoven into the discussion, much of this chapter is devoted to cataloging these solutions. The results are used in this chapter for describing EQS fields in free space. However, as effects of polarization and conduction are added to the EQS purview, and as MQS systems with magnetization and conduction are considered, the homogeneous solutions to Laplace’s equation established in this chapter will be a continual resource.

A review of Chap. 4 will identify many solutions to Laplace’s equation. As long as the field source is outside the region of interest, the resulting potential obeys Laplace’s equation. What is different about the solutions established in this chapter? A hint comes from the numerical procedure used in Sec. 4.8 to satisfy arbitrary boundary conditions. There, a superposition of  $N$  solutions to Laplace’s equation was used to satisfy conditions at  $N$  points on the boundaries. Unfortunately, to determine the amplitudes of these  $N$  solutions,  $N$  equations had to be solved for  $N$  unknowns.

The solutions to Laplace’s equation found in this chapter can also be used as the terms in an infinite series that is made to satisfy arbitrary boundary conditions. But what is different about the terms in this series is their orthogonality. This property of the solutions makes it possible to explicitly determine the individual amplitudes in the series. The notion of the orthogonality of functions may already

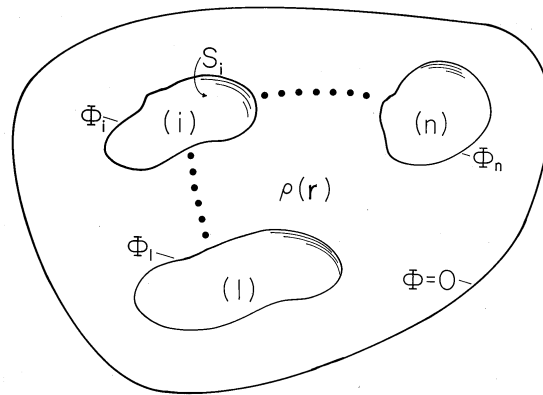


**Fig. 5.1.1** Volume of interest in which there can be a distribution of charge density. To illustrate bounding surfaces on which potential is constrained,  $n$  isolated surfaces and one enclosing surface are shown.

be familiar through an exposure to Fourier analysis. In any case, the fundamental ideas involved are introduced in Sec. 5.5.

## 5.1 PARTICULAR AND HOMOGENEOUS SOLUTIONS TO POISSON'S AND LAPLACE'S EQUATIONS

Suppose we want to analyze an electroquasistatic situation as shown in Fig. 5.1.1. A charge distribution  $\rho(\mathbf{r})$  is specified in the part of space of interest, designated by the volume  $V$ . This region is bounded by perfect conductors of specified shape and location. Known potentials are applied to these conductors and the enclosing surface, which may be at infinity.

In the space between the conductors, the potential function obeys Poisson's equation, (5.0.2). A particular solution of this equation within the prescribed volume  $V$  is given by the superposition integral, (4.5.3).

$$\Phi_p(\mathbf{r}) = \int_{V'} \frac{\rho(\mathbf{r}') dv'}{4\pi\epsilon_0 |\mathbf{r} - \mathbf{r}'|} \quad (1)$$

This potential obeys Poisson's equation at each point within the volume  $V$ . Since we do not evaluate this equation outside the volume  $V$ , the integration over the sources called for in (1) need include no sources other than those within the volume  $V$ . This makes it clear that the particular solution is not unique, because the addition to the potential made by integrating over arbitrary charges outside the volume  $V$  will only give rise to a potential, the Laplacian derivative of which is zero within the volume  $V$ .

Is (1) the complete solution? Because it is not unique, the answer must be, surely not. Further, it is clear that no information as to the position and shape of the conductors is built into this solution. Hence, the electric field obtained as the negative gradient of the potential  $\Phi_p$  of (1) will, in general, possess a finite tangential component on the surfaces of the electrodes. On the other hand, the conductors

have surface charge distributions which adjust themselves so as to cause the net electric field on the surfaces of the conductors to have vanishing tangential electric field components. The distribution of these surface charges is not known at the outset and hence cannot be included in the integral (1).

A way out of this dilemma is as follows: The potential distribution we seek within the space not occupied by the conductors is the result of two charge distributions. First is the prescribed volume charge distribution leading to the potential function  $\Phi_p$ , and second is the charge distributed on the conductor surfaces. The potential function produced by the surface charges must obey the source-free Poisson's equation in the space  $V$  of interest. Let us denote this solution to the homogeneous form of Poisson's equation by the potential function  $\Phi_h$ . Then, in the volume  $V$ ,  $\Phi_h$  must satisfy Laplace's equation.

$$\nabla^2 \Phi_h = 0 \quad (2)$$

The superposition principle then makes it possible to write the total potential as

$$\Phi = \Phi_p + \Phi_h \quad (3)$$

The problem of finding the complete field distribution now reduces to that of finding a solution such that the net potential  $\Phi$  of (3) has the prescribed potentials  $v_i$  on the surfaces  $S_i$ . Now  $\Phi_p$  is known and can be evaluated on the surface  $S_i$ . Evaluation of (3) on  $S_i$  gives

$$v_i = \Phi_p(S_i) + \Phi_h(S_i) \quad (4)$$

so that the homogeneous solution is prescribed on the boundaries  $S_i$ .

$$\Phi_h(S_i) = v_i - \Phi_p(S_i) \quad (5)$$

Hence, the determination of an electroquasistatic field with prescribed potentials on the boundaries is reduced to finding the solution to Laplace's equation, (2), that satisfies the boundary condition given by (5).

The approach which has been formalized in this section is another point of view applicable to the boundary value problems in the last part of Chap. 4. Certainly, the abstract view of the boundary value situation provided by Fig. 5.1.1 is not different from that of Fig. 4.6.1. In Example 4.6.4, the field shown in Fig. 4.6.8 is determined for a point charge adjacent to an equipotential charge-neutral spherical electrode. In the volume  $V$  of interest outside the electrode, the volume charge distribution is singular, the point charge  $q$ . The potential given by (4.6.35), in fact, takes the form of (3). The particular solution can be taken as the first term, the potential of a point charge. The second and third terms, which are equivalent to the potentials caused by the fictitious charges within the sphere, can be taken as the homogeneous solution.

**Superposition to Satisfy Boundary Conditions.** In the following sections, superposition will often be used in another way to satisfy boundary conditions.

Suppose that there is no charge density in the volume  $V$ , and again the potentials on each of the  $n$  surfaces  $S_j$  are  $v_j$ . Then

$$\nabla^2\Phi = 0 \quad (6)$$

$$\Phi = v_j \quad \text{on } S_j, \quad j = 1, \dots, n \quad (7)$$

The solution is broken into a superposition of solutions  $\Phi_j$  that meet the required condition on the  $j$ -th surface but are zero on all of the others.

$$\Phi = \sum_{j=1}^n \Phi_j \quad (8)$$

$$\Phi_j \equiv \begin{cases} v_j & \text{on } S_j \\ 0 & \text{on } S_1 \dots S_{j-1}, S_{j+1} \dots S_n \end{cases} \quad (9)$$

Each term is a solution to Laplace's equation, (6), so the sum is as well.

$$\nabla^2\Phi_j = 0 \quad (10)$$

In Sec. 5.5, a method is developed for satisfying arbitrary boundary conditions on one of four surfaces enclosing a volume of interest.

**Capacitance Matrix.** Suppose that in the  $n$  electrode system the net charge on the  $i$ -th electrode is to be found. In view of (8), the integral of  $\mathbf{E} \cdot d\mathbf{a}$  over the surface  $S_i$  enclosing this electrode then gives

$$q_i = - \oint_{S_i} \epsilon_o \nabla\Phi \cdot d\mathbf{a} = - \oint_{S_i} \epsilon_o \sum_{j=1}^n \nabla\Phi_j \cdot d\mathbf{a} \quad (11)$$

Because of the linearity of Laplace's equation, the potential  $\Phi_j$  is proportional to the voltage exciting that potential,  $v_j$ . It follows that (11) can be written in terms of capacitance parameters that are independent of the excitations. That is, (11) becomes

$$q_i = \sum_{j=1}^n C_{ij} v_j \quad (12)$$

where the *capacitance coefficients* are

$$C_{ij} = \frac{- \oint_{S_i} \epsilon_o \nabla\Phi_j \cdot d\mathbf{a}}{v_j} \quad (13)$$

The charge on the  $i$ -th electrode is a linear superposition of the contributions of all  $n$  voltages. The coefficient multiplying its own voltage,  $C_{ii}$ , is called the *self-capacitance*, while the others,  $C_{ij}$ ,  $i \neq j$ , are the *mutual capacitances*.

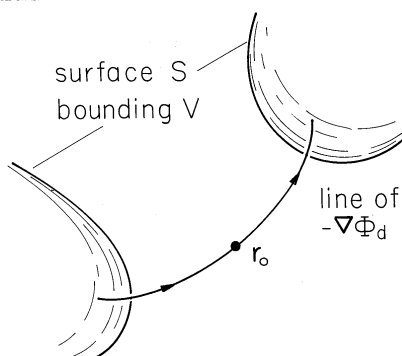


**Fig. 5.2.1** Field line originating on one part of bounding surface and terminating on another after passing through the point  $\mathbf{r}_o$ .

## 5.2 UNIQUENESS OF SOLUTIONS TO POISSON'S EQUATION

We shall show in this section that a potential distribution obeying Poisson's equation is completely specified within a volume  $V$  if the potential is specified over the surfaces bounding that volume. Such a uniqueness theorem is useful for two reasons: (a) It tells us that if we have found such a solution to Poisson's equation, whether by mathematical analysis or physical insight, then we have found the only solution; and (b) it tells us what boundary conditions are appropriate to uniquely specify a solution. If there is no charge present in the volume of interest, then the theorem states the uniqueness of solutions to Laplace's equation.

Following the method "reductio ad absurdum", we assume that the solution is not unique— that two solutions,  $\Phi_a$  and  $\Phi_b$ , exist, satisfying the same boundary conditions— and then show that this is impossible. The presumably different solutions  $\Phi_a$  and  $\Phi_b$  must satisfy Poisson's equation with the same charge distribution and must satisfy the same boundary conditions.

$$\nabla^2 \Phi_a = -\frac{\rho}{\epsilon_o}; \quad \Phi_a = \Phi_i \quad \text{on} \quad S_i \quad (1)$$

$$\nabla^2 \Phi_b = -\frac{\rho}{\epsilon_o}; \quad \Phi_b = \Phi_i \quad \text{on} \quad S_i \quad (2)$$

It follows that with  $\Phi_d$  defined as the difference in the two potentials,  $\Phi_d = \Phi_a - \Phi_b$ ,

$$\nabla^2 \Phi_d \equiv \nabla \cdot (\nabla \Phi_d) = 0; \quad \Phi_d = 0 \quad \text{on} \quad S_i \quad (3)$$

A simple argument now shows that the only way  $\Phi_d$  can both satisfy Laplace's equation and be zero on all of the bounding surfaces is for it to be zero. First, it is argued that  $\Phi_d$  cannot possess a maximum or minimum at any point within  $V$ . With the help of Fig. 5.2.1, visualize the negative of the gradient of  $\Phi_d$ , a field line, as it passes through some point  $\mathbf{r}_o$ . Because the field is solenoidal (divergence free), such a field line cannot start or stop within  $V$  (Sec. 2.7). Further, the field defines a potential (4.1.4). Hence, as one proceeds along the field line in the direction of the negative gradient, the potential has to decrease until the field line reaches one of the surfaces  $S_i$  bounding  $V$ . Similarly, in the opposite direction, the potential has to increase until another one of the surfaces is reached. Accordingly, all maximum and minimum values of  $\Phi_d(\mathbf{r})$  have to be located on the surfaces.

The difference potential at any interior point cannot assume a value larger than or smaller than the largest or smallest value of the potential on the surfaces. But the surfaces are themselves at zero potential. It follows that the difference potential is zero everywhere in  $V$  and that  $\Phi_a = \Phi_b$ . Therefore, only one solution exists to the boundary value problem stated with (1).

### 5.3 CONTINUITY CONDITIONS

At the surfaces of metal conductors, charge densities accumulate that are only a few atomic distances thick. In describing their fields, the details of the distribution within this thin layer are often not of interest. Thus, the charge is represented by a surface charge density (1.3.11) and the surface supporting the charge treated as a surface of discontinuity.

In such cases, it is often convenient to divide a volume in which the field is to be determined into regions separated by the surfaces of discontinuity, and to use piece-wise continuous functions to represent the fields. Continuity conditions are then needed to connect field solutions in two regions separated by the discontinuity. These conditions are implied by the differential equations that apply throughout the region. They assure that the fields are consistent with the basic laws, even in passing through the discontinuity.

Each of the four Maxwell's equations implies a continuity condition. Because of the singular nature of the source distribution, these laws are used in integral form to relate the fields to either side of the surface of discontinuity. With the vector  $\mathbf{n}$  defined as the unit normal to the surface of discontinuity and pointing from region (b) to region (a), the continuity conditions were summarized in Table 1.8.3.

In the EQS approximation, the laws of primary interest are Faraday's law without the magnetic induction and Gauss' law, the first two equations of Chap. 4. Thus, the corresponding EQS continuity conditions are

$$\mathbf{n} \times [\mathbf{E}^a - \mathbf{E}^b] = 0 \quad (1)$$

$$\mathbf{n} \cdot (\epsilon_o \mathbf{E}^a - \epsilon_o \mathbf{E}^b) = \sigma_s \quad (2)$$

Because the magnetic induction makes no contribution to Faraday's continuity condition in any case, these conditions are the same as for the general electrodynamic laws. As a reminder, the contour enclosing the integration surface over which Faraday's law was integrated (Sec. 1.6) to obtain (1) is shown in Fig. 5.3.1a. The integration volume used to obtain (2) from Gauss' law (Sec. 1.3) is similarly shown in Fig. 5.3.1b.

What are the continuity conditions on the electric potential? The potential  $\Phi$  is continuous across a surface of discontinuity even if that surface carries a surface charge density. This will be the case when the  $\mathbf{E}$  field is finite (a dipole layer containing an infinite field causes a jump of potential), because then the line integral of the electric field from one side of the surface to the other side is zero, the path-length being infinitely small.

$$\Phi^a - \Phi^b = 0 \quad (3)$$

To determine the jump condition representing Gauss' law through the surface of discontinuity, it was integrated (Sec. 1.3) over the volume shown intersecting the



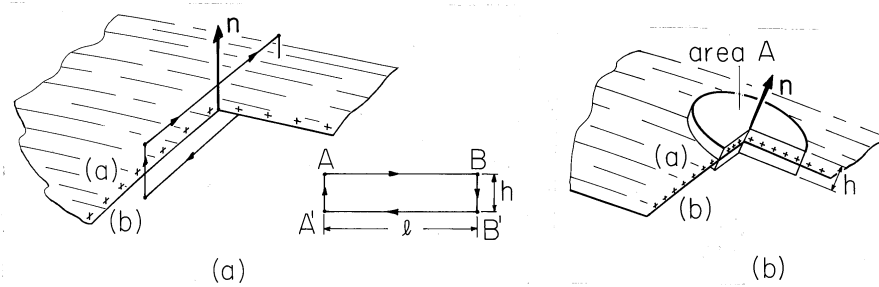


**Fig. 5.3.1** (a) Differential contour intersecting surface supporting surface charge density. (b) Differential volume enclosing surface charge on surface having normal  $\mathbf{n}$ .

surface in Fig. 5.3.1b. The resulting continuity condition, (2), is written in terms of the potential by recognizing that in the EQS approximation,  $\mathbf{E} = -\nabla\Phi$ .

$$\mathbf{n} \cdot [(\nabla\Phi)^a - (\nabla\Phi)^b] = -\frac{\sigma_s}{\epsilon_o} \quad (4)$$

*At a surface of discontinuity that carries a surface charge density, the normal derivative of the potential is discontinuous.*

The continuity conditions become boundary conditions if they are made to represent physical constraints that go beyond those already implied by the laws that prevail in the volume. A familiar example is one where the surface is that of an electrode constrained in its potential. Then the continuity condition (3) requires that the potential in the volume adjacent to the electrode be the given potential of the electrode. This statement cannot be justified without invoking information about the physical nature of the electrode (that it is “infinitely conducting,” for example) that is not represented in the volume laws and hence is not intrinsic to the continuity conditions.

## 5.4 SOLUTIONS TO LAPLACE'S EQUATION IN CARTESIAN COORDINATES

Having investigated some general properties of solutions to Poisson's equation, it is now appropriate to study specific methods of solution to Laplace's equation subject to boundary conditions. Exemplified by this and the next section are three standard steps often used in representing EQS fields. First, Laplace's equation is set up in the coordinate system in which the boundary surfaces are coordinate surfaces. Then, the partial differential equation is reduced to a set of ordinary differential equations by separation of variables. In this way, an infinite set of solutions is generated. Finally, the boundary conditions are satisfied by superimposing the solutions found by separation of variables.

In this section, solutions are derived that are natural if boundary conditions are stated along coordinate surfaces of a Cartesian coordinate system. It is assumed that the fields depend on only two coordinates,  $x$  and  $y$ , so that Laplace's equation

is (Table I)

$$\frac{\partial^2 \Phi}{\partial x^2} + \frac{\partial^2 \Phi}{\partial y^2} = 0 \quad (1)$$

This is a partial differential equation in two independent variables. One time-honored method of mathematics is to reduce a new problem to a problem previously solved. Here the process of finding solutions to the partial differential equation is reduced to one of finding solutions to ordinary differential equations. This is accomplished by the *method of separation of variables*. It consists of assuming solutions with the special space dependence

$$\Phi(x, y) = X(x)Y(y) \quad (2)$$

In (2),  $X$  is assumed to be a function of  $x$  alone and  $Y$  is a function of  $y$  alone. If need be, a general space dependence is then recovered by superposition of these special solutions. Substitution of (2) into (1) and division by  $\Phi$  then gives

$$\frac{1}{X(x)} \frac{d^2 X(x)}{dx^2} = -\frac{1}{Y(y)} \frac{d^2 Y(y)}{dy^2} \quad (3)$$

Total derivative symbols are used because the respective functions  $X$  and  $Y$  are by definition only functions of  $x$  and  $y$ .

In (3) we now have on the left-hand side a function of  $x$  alone, on the right-hand side a function of  $y$  alone. The equation can be satisfied independent of  $x$  and  $y$  only if each of these expressions is constant. We denote this "separation" constant by  $k^2$ , and it follows that

$$\frac{d^2 X}{dx^2} = -k^2 X \quad (4)$$

and

$$\frac{d^2 Y}{dy^2} = k^2 Y \quad (5)$$

These equations have the solutions

$$X \sim \cos kx \quad \text{or} \quad \sin kx \quad (6)$$

$$Y \sim \cosh ky \quad \text{or} \quad \sinh ky \quad (7)$$

If  $k = 0$ , the solutions degenerate into

$$X \sim \text{constant} \quad \text{or} \quad x \quad (8)$$

$$Y \sim \text{constant} \quad \text{or} \quad y \quad (9)$$

The product solutions, (2), are summarized in the first four rows of Table 5.4.1. Those in the right-hand column are simply those of the middle column with the roles of  $x$  and  $y$  interchanged. Generally, we will leave the prime off the  $k'$  in writing these solutions. Exponentials are also solutions to (7). These, sometimes more convenient, solutions are summarized in the last four rows of the table.

The solutions summarized in this table can be used to gain insight into the nature of EQS fields. A good investment is therefore made if they are now visualized.

The fields represented by the potentials in the left-hand column of Table 5.4.1 are all familiar. Those that are linear in  $x$  and  $y$  represent uniform fields, in the  $x$  and  $y$  directions, respectively. The potential  $xy$  is familiar from Fig. 4.1.3. We will use similar conventions to represent the potentials of the second column, but it is helpful to have in mind the three-dimensional portrayal exemplified for the potential  $xy$  in Fig. 4.1.4. In the more complicated field maps to follow, the sketch is visualized as a contour map of the potential  $\Phi$  with peaks of positive potential and valleys of negative potential.

On the top and left peripheries of Fig. 5.4.1 are sketched the functions  $\cos kx$  and  $\cosh ky$ , respectively, the product of which is the first of the potentials in the middle column of Table 5.4.1. If we start out from the origin in either the  $+y$  or  $-y$  directions (north or south), we climb a potential hill. If we instead proceed in the  $+x$  or  $-x$  directions (east or west), we move downhill. An easterly path begun on the potential hill to the north of the origin corresponds to a decrease in the  $\cos kx$  factor. To follow a path of equal elevation, the  $\cosh ky$  factor must increase, and this implies that the path must turn northward.

A good starting point in making these field sketches is the identification of the contours of zero potential. In the plot of the second potential in the middle column of Table 5.4.1, shown in Fig. 5.4.2, these are the  $y$  axis and the lines  $kx = +\pi/2, +3\pi/2, \text{etc.}$  The dependence on  $y$  is now odd rather than even, as it was for the plot of Fig. 5.4.1. Thus, the origin is now on the side of a potential hill that slopes downward from north to south.

The solutions in the third and fourth rows of the second column possess the same field patterns as those just discussed provided those patterns are respectively shifted in the  $x$  direction. In the last four rows of Table 5.4.1 are four additional possible solutions which are linear combinations of the previous four in that column. Because these decay exponentially in either the  $+y$  or  $-y$  directions, they are useful for representing solutions in problems where an infinite half-space is considered.

The solutions in Table 5.4.1 are nonsingular throughout the entire  $x-y$  plane. This means that Laplace's equation is obeyed everywhere within the finite  $x-y$  plane, and hence the field lines are continuous; they do not appear or disappear. The sketches show that the fields become stronger and stronger as one proceeds in the positive and negative  $y$  directions. The lines of electric field originate on positive charges and terminate on negative charges at  $y \rightarrow \pm\infty$ . Thus, for the plots shown in Figs. 5.4.1 and 5.4.2, the charge distributions at infinity must consist of alternating distributions of positive and negative charges of infinite amplitude.

Two final observations serve to further develop an appreciation for the nature of solutions to Laplace's equation. First, the third dimension can be used to represent the potential in the manner of Fig. 4.1.4, so that the potential surface has the shape of a membrane stretched from boundaries that are elevated in proportion to their potentials.

Laplace's equation, (1), requires that the sum of quantities that reflect the curvatures in the  $x$  and  $y$  directions vanish. If the second derivative of a function is positive, it is curved upward; and if it is negative, it is curved downward. If the curvature is positive in the  $x$  direction, it must be negative in the  $y$  direction. Thus, at the origin in Fig. 5.4.1, the potential is cupped downward for excursions in the

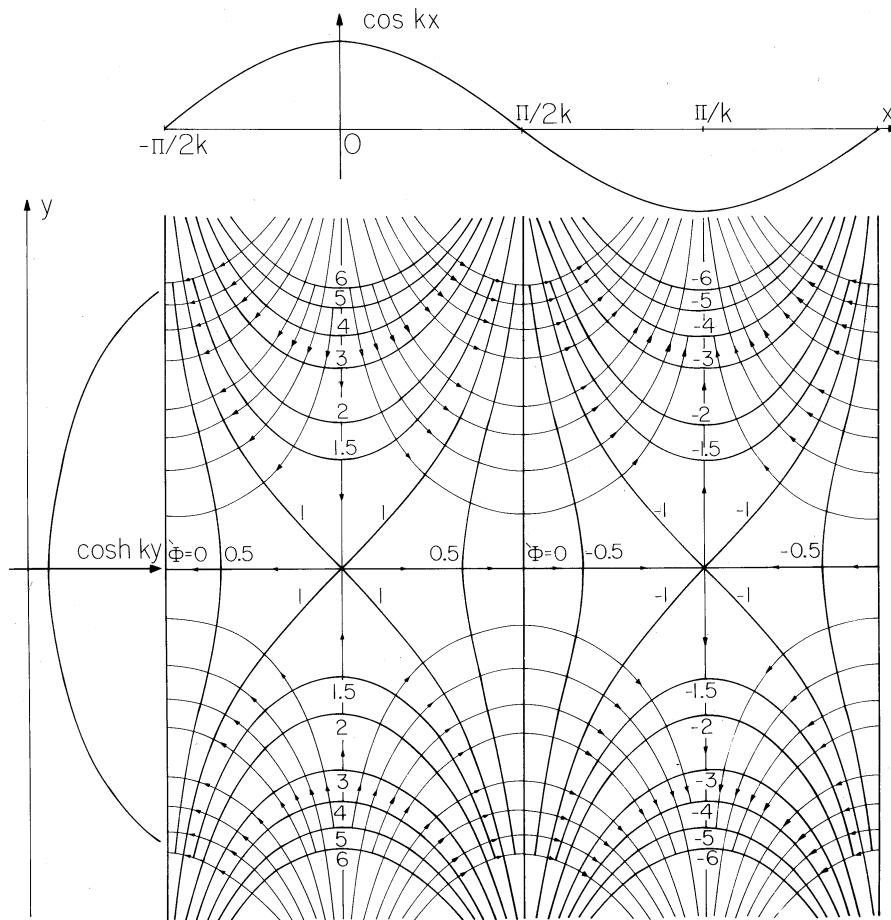


**Fig. 5.4.1** Equipotentials for  $\Phi = \cos(kx) \cosh(ky)$  and field lines. As an aid to visualizing the potential, the separate factors  $\cos(kx)$  and  $\cosh(ky)$  are, respectively, displayed at the top and to the left.

$x$  direction, and so it must be cupped upward for variations in the  $y$  direction. A similar deduction must apply at every point in the  $x - y$  plane.

Second, because the  $k$  that appears in the periodic functions of the second column in Table 5.4.1 is the same as that in the exponential and hyperbolic functions, it is clear that the more rapid the periodic variation, the more rapid is the decay or apparent growth.

### 5.5 MODAL EXPANSION TO SATISFY BOUNDARY CONDITIONS

Each of the solutions obtained in the preceding section by separation of variables could be produced by an appropriate potential applied to pairs of parallel surfaces

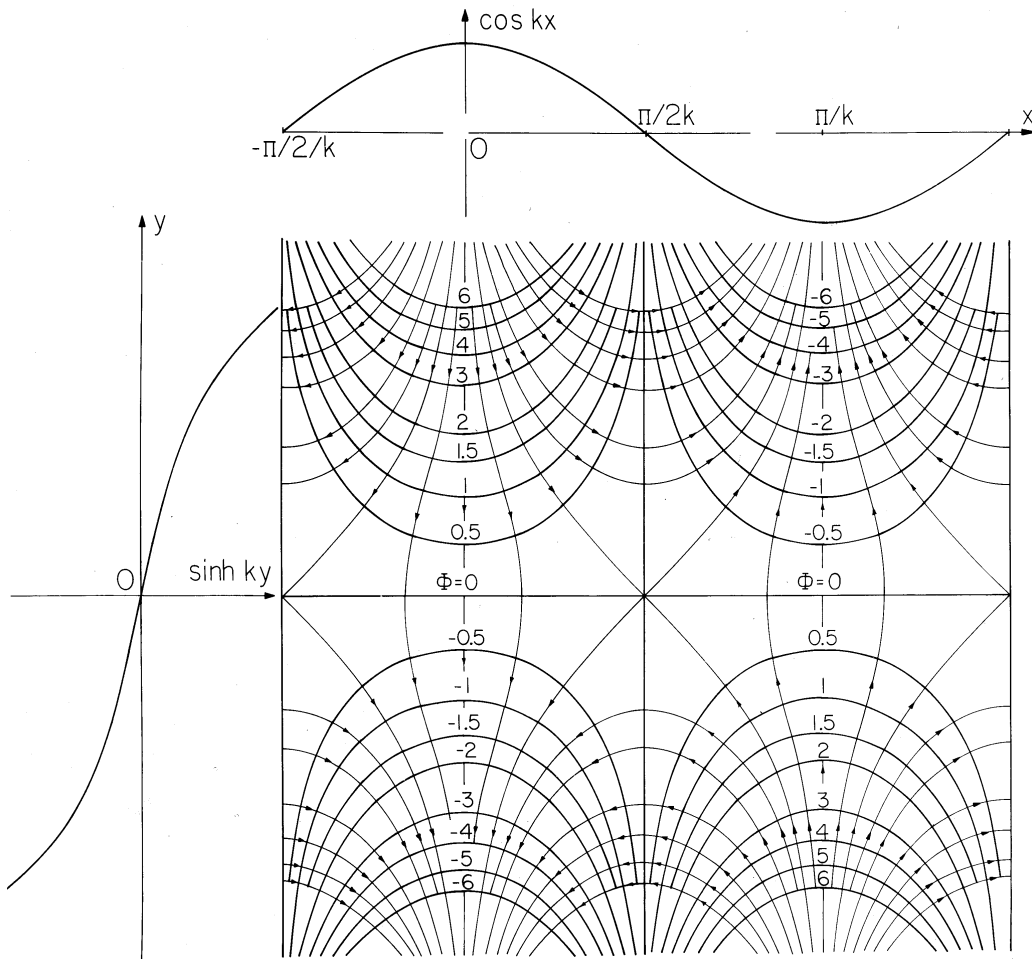


**Fig. 5.4.2** Equipotentials for  $\Phi = \cos(kx)\sinh(ky)$  and field lines. As an aid to visualizing the potential, the separate factors  $\cos(kx)$  and  $\sinh(ky)$  are, respectively, displayed at the top and to the left.

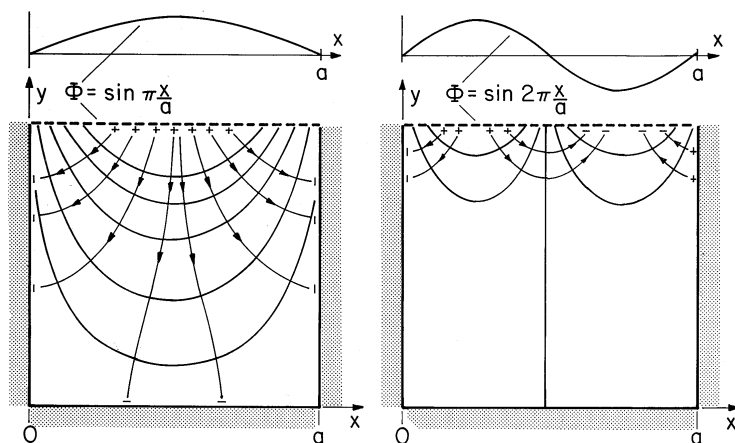
in the planes  $x = \text{constant}$  and  $y = \text{constant}$ . Consider, for example, the fourth solution in the column  $k^2 \geq 0$  of Table 5.4.1, which with a constant multiplier is

$$\Phi = A \sin kx \sinh ky \tag{1}$$

This solution has  $\Phi = 0$  in the plane  $y = 0$  and in the planes  $x = n\pi/k$ , where  $n$  is an integer. Suppose that we set  $k = n\pi/a$  so that  $\Phi = 0$  in the plane  $y = a$  as well. Then at  $y = b$ , the potential of (1)

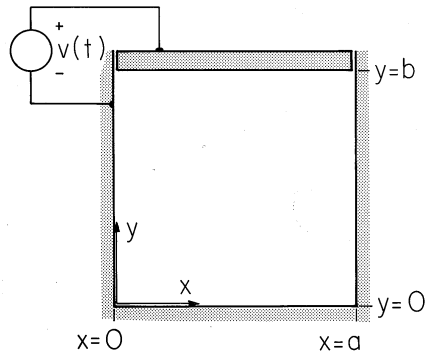
$$\Phi(x, b) = A \sinh \frac{n\pi}{a} b \sin \frac{n\pi}{a} x \tag{2}$$

TABLE 5.4.1		
TWO-DIMENSIONAL CARTESIAN SOLUTIONS		
OF LAPLACE'S EQUATION		
$k = 0$	$k^2 \geq 0$	$k^2 \leq 0 (k \rightarrow jk')$
Constant	$\cos kx \cosh ky$	$\cosh k'x \cos k'y$
$y$	$\cos kx \sinh ky$	$\cosh k'x \sin k'y$
$x$	$\sin kx \cosh ky$	$\sinh k'x \cos k'y$
$xy$	$\sin kx \sinh ky$	$\sinh k'x \sin k'y$
	$\cos kx e^{ky}$	$e^{k'x} \cos k'y$
	$\cos kx e^{-ky}$	$e^{-k'x} \cos k'y$
	$\sin kx e^{ky}$	$e^{k'x} \sin k'y$
	$\sin kx e^{-ky}$	$e^{-k'x} \sin k'y$



**Fig. 5.5.1** Two of the infinite number of potential functions having the form of (1) that will fit the boundary conditions  $\Phi = 0$  at  $y = 0$  and at  $x = 0$  and  $x = a$ .

has a sinusoidal dependence on  $x$ . If a potential of the form of (2) were applied along the surface at  $y = b$ , and the surfaces at  $x = 0$ ,  $x = a$ , and  $y = 0$  were held at zero potential (by, say, planar conductors held at zero potential), then the potential, (1), would exist within the space  $0 < x < a$ ,  $0 < y < b$ . Segmented electrodes having each segment constrained to the appropriate potential could be used to approximate the distribution at  $y = b$ . The potential and field plots for  $n = 1$  and  $n = 2$  are given in Fig. 5.5.1. Note that the theorem of Sec. 5.2 insures



**Fig. 5.5.2** Cross-section of zero-potential rectangular slot with an electrode having the potential  $v$  inserted at the top.

that the specified potential is unique.

But what can be done to describe the field if the wall potentials are not constrained to fit neatly the solution obtained by separation of variables? For example, suppose that the fields are desired in the same region of rectangular cross-section, but with an electrode at  $y = b$  constrained to have a potential  $v$  that is independent of  $x$ . The configuration is now as shown in Fig. 5.5.2.

A line of attack is suggested by the infinite number of solutions, having the form of (1), that meet the boundary condition on three of the four walls. The superposition principle makes it clear that any linear combination of these is also a solution, so if we let  $A_n$  be arbitrary coefficients, a more general solution is

$$\Phi = \sum_{n=1}^{\infty} A_n \sinh \frac{n\pi}{a} y \sin \frac{n\pi}{a} x \quad (3)$$

Note that  $k$  has been assigned values such that the sine function is zero in the planes  $x = 0$  and  $x = a$ . Now how can we adjust the coefficients so that the boundary condition at the driven electrode, at  $y = b$ , is met? One approach that we will not have to use is suggested by the numerical method described in Sec. 4.8. The electrode could be divided into  $N$  segments and (3) evaluated at the center point of each of the segments. If the infinite series were truncated at  $N$  terms, the result would be  $N$  equations that were linear in the  $N$  unknowns  $A_n$ . This system of equations could be inverted to determine the  $A_n$ 's. Substitution of these into (3) would then comprise a solution to the boundary value problem. Unfortunately, to achieve reasonable accuracy, large values of  $N$  would be required and a computer would be needed.

The power of the approach of variable separation is that it results in solutions that are orthogonal in a sense that makes it possible to determine explicitly the coefficients  $A_n$ . The evaluation of the coefficients is remarkably simple. First, (3) is evaluated on the surface of the electrode where the potential is known.

$$\Phi(x, b) = \sum_{n=1}^{\infty} A_n \sinh \frac{n\pi b}{a} \sin \frac{n\pi}{a} x \quad (4)$$

On the right is the infinite series of sinusoidal functions with coefficients that are to be determined. On the left is a given function of  $x$ . We multiply both sides of the expression by  $\sin(m\pi x/a)$ , where  $m$  is one integer, and then both sides of the expression are integrated over the width of the system.

$$\int_0^a \Phi(x, b) \sin \frac{m\pi}{a} x dx = \sum_{n=1}^{\infty} A_n \sinh \frac{n\pi b}{a} \int_0^a \sin \frac{m\pi}{a} x \sin \frac{n\pi}{a} x dx \quad (5)$$

The functions  $\sin(n\pi x/a)$  and  $\sin(m\pi x/a)$  are orthogonal in the sense that the integral of their product over the specified interval is zero, unless  $m = n$ .

$$\int_0^a \sin \frac{m\pi}{a} x \sin \frac{n\pi}{a} x dx = \begin{cases} 0, & n \neq m \\ \frac{a}{2}, & n = m \end{cases} \quad (6)$$

Thus, all the terms on the right in (5) vanish, except the one having  $n = m$ . Of course,  $m$  can be any integer, so we can solve (5) for the  $m$ -th amplitude and then replace  $m$  by  $n$ .

$$A_n = \frac{2}{a \sinh \frac{n\pi b}{a}} \int_0^a \Phi(x, b) \sin \frac{n\pi}{a} x dx \quad (7)$$

Given any distribution of potential on the surface  $y = b$ , this integral can be carried out and hence the coefficients determined. In this specific problem, the potential is  $v$  at each point on the electrode surface. Thus, (7) is evaluated to give

$$A_n = \frac{2v(t)}{n\pi} \frac{(1 - \cos \pi n)}{\sinh \left( \frac{n\pi b}{a} \right)} = \begin{cases} 0; & n \text{ even} \\ \frac{4v}{n\pi} \frac{1}{\sinh \left( \frac{n\pi b}{a} \right)}; & n \text{ odd} \end{cases} \quad (8)$$

Finally, substitution of these coefficients into (3) gives the desired potential.

$$\Phi = \sum_{\substack{n=1 \\ \text{odd}}}^{\infty} \frac{4v(t)}{\pi} \frac{1}{n} \frac{\sinh \left( \frac{n\pi}{a} y \right)}{\sinh \left( \frac{n\pi b}{a} \right)} \sin \frac{n\pi}{a} x \quad (9)$$

Each product term in this infinite series satisfies Laplace's equation and the zero potential condition on three of the surfaces enclosing the region of interest. The *sum* satisfies the potential condition on the "last" boundary. Note that the sum is not itself in the form of the product of a function of  $x$  alone and a function of  $y$  alone.

The modal expansion is applicable with an arbitrary distribution of potential on the "last" boundary. But what if we have an arbitrary distribution of potential on all four of the planes enclosing the region of interest? The superposition principle justifies using the sum of four solutions of the type illustrated here. Added to the series solution already found are three more, each analogous to the previous one, but rotated by 90 degrees. Because each of the four series has a finite potential only on the part of the boundary to which its series applies, the sum of the four satisfy all boundary conditions.

The potential given by (9) is illustrated in Fig. 5.5.3. In the three-dimensional portrayal, it is especially clear that the field is infinitely large in the corners where



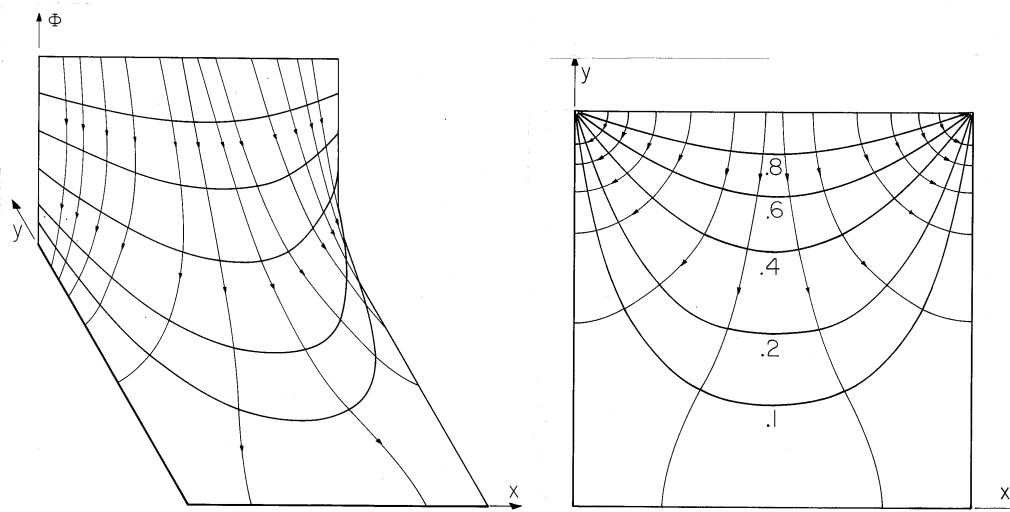


**Fig. 5.5.3** Potential and field lines for the configuration of Fig. 5.5.2, (9), shown using vertical coordinate to display the potential and shown in  $x - y$  plane.

the driven electrode meets the grounded walls. Where the electric field emanates from the driven electrode, there is surface charge, so at the corners there is an infinite surface charge density. In practice, of course, the spacing is not infinitesimal and the fields are not infinite.

### Demonstration 5.5.1. Capacitance Attenuator

Because neither of the field laws in this chapter involve time derivatives, the field that has been determined is correct for  $v = v(t)$ , an arbitrary function of time. As a consequence, the coefficients  $A_n$  are also functions of time. Thus, the charges induced on the walls of the box are time varying, as can be seen if the wall at  $y = 0$  is isolated from the grounded side walls and connected to ground through a resistor. The configuration is shown in cross-section by Fig. 5.5.4. The resistance  $R$  is small enough so that the potential  $v_o$  is small compared with  $v$ .

The charge induced on this output electrode is found by applying Gauss' integral law with an integration surface enclosing the electrode. The width of the electrode in the  $z$  direction is  $w$ , so

$$q = \oint_S \epsilon_o \mathbf{E} \cdot d\mathbf{a} = \epsilon_o w \int_0^a E_y(x, 0) dx = -\epsilon_o w \int_0^a \frac{\partial \Phi}{\partial y}(x, 0) dx \quad (10)$$

This expression is evaluated using (9).

$$q = -C_m v; \quad C_m \equiv \frac{8\epsilon_o w}{\pi} \sum_{\substack{n=1 \\ \text{odd}}}^{\infty} \frac{1}{n \sinh\left(\frac{n\pi b}{a}\right)} \quad (11)$$

Conservation of charge requires that the current through the resistance be the rate of change of this charge with respect to time. Thus, the output voltage is

$$v_o = -R \frac{dq}{dt} = RC_m \frac{dv}{dt} \quad (12)$$

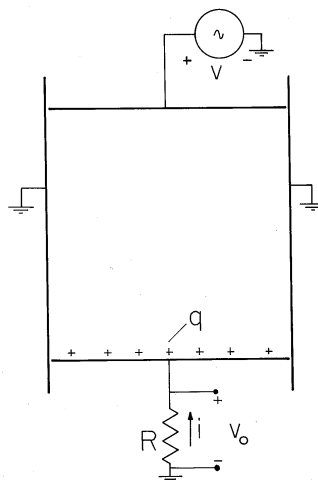


**Fig. 5.5.4** The bottom of the slot is replaced by an insulating electrode connected to ground through a low resistance so that the induced current can be measured.

and if  $v = V \sin \omega t$ , then

$$v_o = RC_m \omega V \cos \omega t \equiv V_o \cos \omega t \quad (13)$$

The experiment shown in Fig. 5.5.5 is designed to demonstrate the dependence of the output voltage on the spacing  $b$  between the input and output electrodes. It follows from (13) and (11) that this voltage can be written in normalized form as

$$\frac{V_o}{U} = \sum_{\substack{n=1 \\ \text{odd}}}^{\infty} \frac{1}{2n \sinh\left(\frac{n\pi b}{a}\right)}; \quad U \equiv \frac{16\epsilon_o w \omega R}{\pi} V \quad (14)$$

Thus, the natural log of the normalized voltage has the dependence on the electrode spacing shown in Fig. 5.5.5. Note that with increasing  $b/a$  the function quickly becomes a straight line. In the limit of large  $b/a$ , the hyperbolic sine can be approximated by  $\exp(n\pi b/a)/2$  and the series can be approximated by one term. Thus, the dependence of the output voltage on the electrode spacing becomes simply

$$\ln\left(\frac{V_o}{U}\right) = \ln e^{-(\pi b/a)} = -\pi \frac{b}{a} \quad (15)$$

and so the asymptotic slope of the curve is  $-\pi$ .

Charges induced on the input electrode have their images either on the side walls of the box or on the output electrode. If  $b/a$  is small, almost all of these images are on the output electrode, but as it is withdrawn, more and more of the images are on the side walls and fewer are on the output electrode.

In retrospect, there are several matters that deserve further discussion. First, the potential used as a starting point in this section, (1), is one from a list of four in Table 5.4.1. What type of procedure can be used to select the appropriate form? In general, the solution used to satisfy the zero potential boundary condition on the

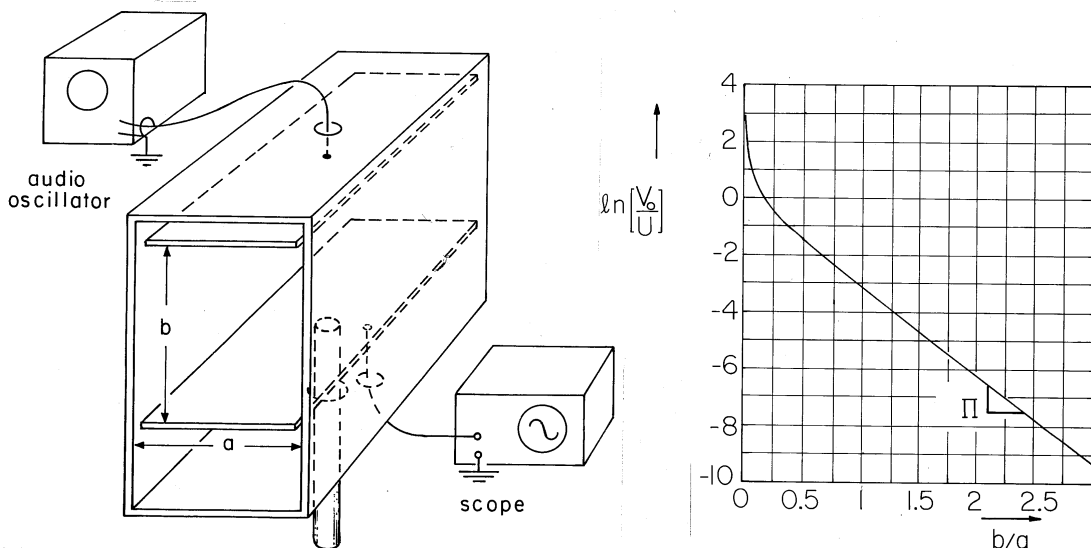


**Fig. 5.5.5** Demonstration of electroquasistatic attenuator in which normalized output voltage is measured as a function of the distance between input and output electrodes normalized to the smaller dimension of the box. The normalizing voltage  $U$  is defined by (14). The output electrode is positioned by means of the attached insulating rod. In operation, a metal lid covers the side of the box.

“first” three surfaces is a linear combination of the four possible solutions. Thus, with the  $A$ 's denoting undetermined coefficients, the general form of the solution is

$$\begin{aligned} \Phi = & A_1 \cos kx \cosh ky + A_2 \cos kx \sinh ky \\ & + A_3 \sin kx \cosh ky + A_4 \sin kx \sinh ky \end{aligned} \tag{16}$$

Formally, (1) was selected by eliminating three of these four coefficients. The first two must vanish because the function must be zero at  $x = 0$ . The third is excluded because the potential must be zero at  $y = 0$ . Thus, we are led to the last term, which, if  $A_4 = A$ , is (1).

The methodical elimination of solutions is necessary. Because the origin of the coordinates is arbitrary, setting up a simple expression for the potential is a matter of choosing the origin of coordinates properly so that as many of the solutions (16) are eliminated as possible. We purposely choose the origin so that a single term from the four in (16) meets the boundary condition at  $x = 0$  and  $y = 0$ . The selection of product solutions from the list should interplay with the choice of coordinates. Some combinations are much more convenient than others. This will be exemplified in this and the following chapters.

The remainder of this section is devoted to a more detailed discussion of the expansion in sinusoids represented by (9). In the plane  $y = b$ , the potential distribution is of the form

$$\Phi(x, b) = \sum_{n=1}^{\infty} V_n \sin \frac{n\pi}{a} x \tag{17}$$

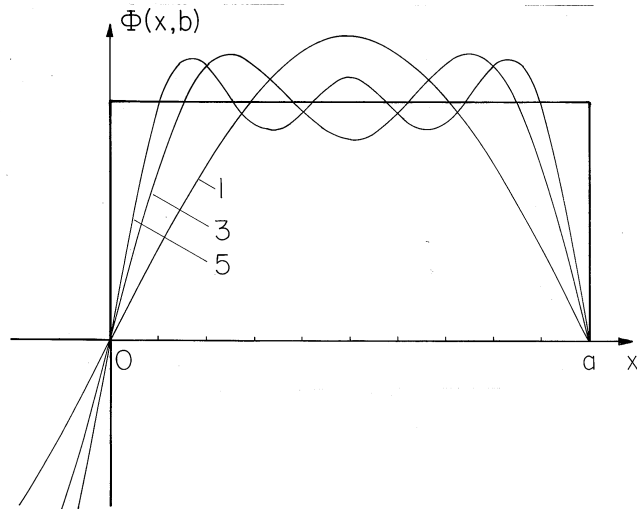


**Fig. 5.5.6** Fourier series approximation to square wave given by (17) and (18), successively showing one, two, and three terms. Higher-order terms tend to fill in the sharp discontinuity at  $x = 0$  and  $x = a$ . Outside the range of interest, the series represents an odd function of  $x$  having a periodicity length  $2a$ .

where the procedure for determining the coefficients has led to (8), written here in terms of the coefficients  $V_n$  of (17) as

$$V_n = \begin{cases} 0, & n \text{ even} \\ \frac{4v}{n\pi}, & n \text{ odd} \end{cases} \quad (18)$$

The approximation to the potential  $v$  that is uniform over the span of the driving electrode is shown in Fig. 5.5.6. Equation (17) represents a square wave of period  $2a$  extending over all  $x$ ,  $-\infty < x < +\infty$ . One half of a period appears as shown in the figure. It is possible to represent this distribution in terms of sinusoids alone because it is odd in  $x$ . In general, a periodic function is represented by a Fourier series of both sines and cosines. In the present problem, cosines were missing because the potential had to be zero at  $x = 0$  and  $x = a$ . Study of a Fourier series shows that the series converges to the actual function in the sense that in the limit of an infinite number of terms,

$$\int_0^a [\Phi^2(x) - F^2(x)] dx = 0 \quad (19)$$

where  $\Phi(x)$  is the actual potential distribution and  $F(x)$  is the Fourier series approximation.

To see the generality of the approach exemplified here, we show that the orthogonality property of the functions  $X(x)$  results from the differential equation and boundary conditions. Thus, it should not be surprising that the solutions in other coordinate systems also have an orthogonality property.

In all cases, the orthogonality property is associated with any one of the factors in a product solution. For the Cartesian problem considered here, it is  $X(x)$  that satisfies boundary conditions at two points in space. This is assured by adjusting

the eigenvalue  $k_n = n\pi/a$  so that the eigenfunction or mode,  $\sin(n\pi x/a)$ , is zero at  $x = 0$  and  $x = a$ . This function satisfies (5.4.4) and the boundary conditions.

$$\frac{d^2 X_m}{dx^2} + k_m^2 X_m = 0; \quad X_m = 0 \quad \text{at} \quad x = 0, a \quad (20)$$

The subscript  $m$  is used to recognize that there is an infinite number of solutions to this problem. Another solution, say the  $n$ -th, must also satisfy this equation and the boundary conditions.

$$\frac{d^2 X_n}{dx^2} + k_n^2 X_n = 0; \quad X_n = 0 \quad \text{at} \quad x = 0, a \quad (21)$$

The orthogonality property for these modes, exploited in evaluating the coefficients of the series expansion, is

$$\int_0^a X_m X_n dx = 0, \quad n \neq m \quad (22)$$

To prove this condition in general, we multiply (20) by  $X_n$  and integrate between the points where the boundary conditions apply.

$$\int_0^a X_n \frac{d}{dx} \left( \frac{dX_m}{dx} \right) dx + \int_0^a k_m^2 X_m X_n dx = 0 \quad (23)$$

By identifying  $u = X_n$  and  $v = dX_m/dx$ , the first term is integrated by parts to obtain

$$\int_0^a X_n \frac{d}{dx} \left( \frac{dX_m}{dx} \right) dx = X_n \frac{dX_m}{dx} \Big|_0^a - \int_0^a \frac{dX_n}{dx} \frac{dX_m}{dx} dx \quad (24)$$

The first term on the right vanishes because of the boundary conditions. Thus, (23) becomes

$$- \int_0^a \frac{dX_m}{dx} \frac{dX_n}{dx} dx + k_m^2 \int_0^a X_m X_n dx = 0 \quad (25)$$

If these same steps are completed with  $n$  and  $m$  interchanged, the result is (25) with  $n$  and  $m$  interchanged. Because the first term in (25) is the same as its counterpart in this second equation, subtraction of the two expressions yields

$$(k_m^2 - k_n^2) \int_0^a X_m X_n dx = 0 \quad (26)$$

Thus, the functions are orthogonal provided that  $k_n \neq k_m$ . For this specific problem, the eigenfunctions are  $X_n = \sin(n\pi/a)$  and the eigenvalues are  $k_n = n\pi/a$ . But in general we can expect that our product solutions to Laplace's equation in other coordinate systems will result in a set of functions having similar orthogonality properties.

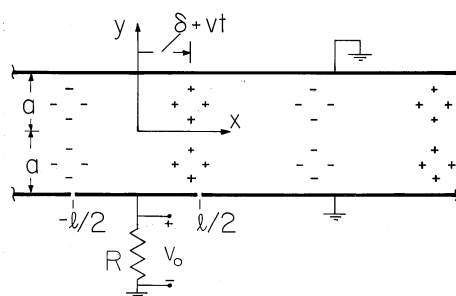


**Fig. 5.6.1** Cross-section of layer of charge that is periodic in the  $x$  direction and bounded from above and below by zero potential plates. With this charge translating to the right, an insulated electrode inserted in the lower equipotential is used to detect the motion.

### 5.6 SOLUTIONS TO POISSON'S EQUATION WITH BOUNDARY CONDITIONS

An approach to solving Poisson's equation in a region bounded by surfaces of known potential was outlined in Sec. 5.1. The potential was divided into a particular part, the Laplacian of which balances  $-\rho/\epsilon_o$  throughout the region of interest, and a homogeneous part that makes the sum of the two potentials satisfy the boundary conditions. In short,

$$\Phi = \Phi_p + \Phi_h \tag{1}$$

$$\nabla^2 \Phi_p = -\frac{\rho}{\epsilon_o} \tag{2}$$

$$\nabla^2 \Phi_h = 0 \tag{3}$$

and on the enclosing surfaces,

$$\Phi_h = \Phi - \Phi_p \quad \text{on } S \tag{4}$$

The following examples illustrate this approach. At the same time they demonstrate the use of the Cartesian coordinate solutions to Laplace's equation and the idea that the fields described can be time varying.

**Example 5.6.1.** Field of Traveling Wave of Space Charge between Equipotential Surfaces

The cross-section of a two-dimensional system that stretches to infinity in the  $x$  and  $z$  directions is shown in Fig. 5.6.1. Conductors in the planes  $y = a$  and  $y = -a$  bound the region of interest. Between these planes the charge density is periodic in the  $x$  direction and uniformly distributed in the  $y$  direction.

$$\rho = \rho_o \cos \beta x \tag{5}$$

The parameters  $\rho_o$  and  $\beta$  are given constants. For now, the segment connected to ground through the resistor in the lower electrode can be regarded as being at the same zero potential as the remainder of the electrode in the plane  $x = -a$  and the electrode in the plane  $y = a$ . First we ask for the field distribution.

Remember that any particular solution to (2) will do. Because the charge density is independent of  $y$ , it is natural to look for a particular solution with the same property. Then, on the left in (2) is a second derivative with respect to  $x$ , and the equation can be integrated twice to obtain

$$\Phi_p = \frac{\rho_o}{\epsilon_o \beta^2} \cos \beta x \quad (6)$$

This particular solution is independent of  $y$ . Note that it is not the potential that would be obtained by evaluating the superposition integral over the charge between the grounded planes. Viewed over all space, that charge distribution is not independent of  $y$ . In fact, the potential of (6) is associated with a charge distribution as given by (5) that extends to infinity in the  $+y$  and  $-y$  directions.

The homogeneous solution must make up for the fact that (6) does not satisfy the boundary conditions. That is, at the boundaries,  $\Phi = 0$  in (1), so the homogeneous and particular solutions must balance there.

$$\Phi_h \Big|_{y=\pm a} = -\Phi_p \Big|_{y=\pm a} = -\frac{\rho_o}{\epsilon_o \beta^2} \cos \beta x \quad (7)$$

Thus, we are looking for a solution to Laplace's equation, (3), that satisfies these boundary conditions. Because the potential has the same value on the boundaries, and the origin of the  $y$  axis has been chosen to be midway between, it is clear that the potential must be an even function of  $y$ . Further, it must have a periodicity in the  $x$  direction that matches that of (7). Thus, from the list of solutions to Laplace's equation in Cartesian coordinates in the middle column of Table 5.4.1,  $k = \beta$ , the  $\sin kx$  terms are eliminated in favor of the  $\cos kx$  solutions, and the  $\cosh ky$  solution is selected because it is even in  $y$ .

$$\Phi_h = A \cosh \beta y \cos \beta x \quad (8)$$

The coefficient  $A$  is now adjusted so that the boundary conditions are satisfied by substituting (8) into (7).

$$A \cosh \beta a \cos \beta x = -\frac{\rho_o}{\epsilon_o \beta^2} \cos \beta x \rightarrow A = -\frac{\rho_o}{\epsilon_o \beta^2 \cosh \beta a} \quad (9)$$

Superposition of the particular solution, (7), and the homogeneous solution given by substituting the coefficient of (9) into (8), results in the desired potential distribution.

$$\Phi = \frac{\rho_o}{\epsilon_o \beta^2} \left( 1 - \frac{\cosh \beta y}{\cosh \beta a} \right) \cos \beta x \quad (10)$$

The mathematical solutions used in deriving (10) are illustrated in Fig. 5.6.2. The particular solution describes an electric field that originates in regions of positive charge density and terminates in regions of negative charge density. It is purely  $x$  directed and is therefore tangential to the equipotential boundary. The homogeneous solution that is added to this field is entirely due to surface charges. These give rise to a field that bucks out the tangential field at the walls, rendering them surfaces of constant potential. Thus, the sum of the solutions (also shown in the figure), satisfies Gauss' law and the boundary conditions.

With this static view of the fields firmly in mind, suppose that the charge distribution is moving in the  $x$  direction with the velocity  $v$ .

$$\rho = \rho_o \cos \beta(x - vt) \quad (11)$$

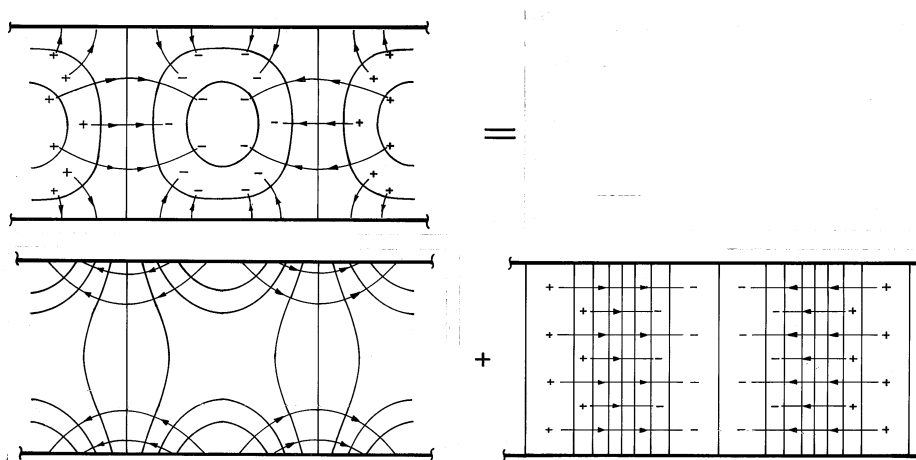


**Fig. 5.6.2** Equipotentials and field lines for configuration of Fig. 5.6.1 showing graphically the superposition of particular and homogeneous parts that gives the required potential.

The variable  $x$  in (5) has been replaced by  $x - vt$ . With this moving charge distribution, the field also moves. Thus, (10) becomes

$$\Phi = \frac{\rho_o}{\epsilon_o \beta^2} \left( 1 - \frac{\cosh \beta y}{\cosh \beta a} \right) \cos \beta(x - vt) \quad (12)$$

Note that the homogeneous solution is now a linear combination of the first and third solutions in the middle column of Table 5.4.1.

As the space charge wave moves by, the charges induced on the perfectly conducting walls follow along in synchronism. The current that accompanies the redistribution of surface charges is detected if a section of the wall is insulated from the rest and connected to ground through a resistor, as shown in Fig. 5.6.1. Under the assumption that the resistance is small enough so that the segment remains at essentially zero potential, what is the output voltage  $v_o$ ?

The current through the resistor is found by invoking charge conservation for the segment to find the current that is the time rate of change of the net charge on the segment. The latter follows from Gauss' integral law and (12) as

$$\begin{aligned} q &= w \int_{-l/2}^{l/2} \epsilon_o E_y \Big|_{y=-a} dx \\ &= -\frac{w \rho_o}{\beta^2} \tanh \beta a \left[ \sin \beta \left( \frac{l}{2} - vt \right) \right. \\ &\quad \left. + \sin \beta \left( \frac{l}{2} + vt \right) \right] \end{aligned} \quad (13)$$

It follows that the dynamics of the traveling wave of space charge is reflected in a measured voltage of

$$v_o = -R \frac{dq}{dt} = -\frac{2Rw\rho_o v}{\beta} \tanh \beta a \sin \frac{\beta l}{2} \sin \beta vt \quad (14)$$



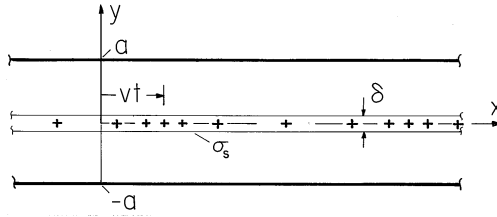


**Fig. 5.6.3** Cross-section of sheet beam of charge between plane parallel equipotential plates. Beam is modeled by surface charge density having dc and ac parts.

In writing this expression, the double-angle formulas have been invoked.

Several predictions should be consistent with intuition. The output voltage varies sinusoidally with time at a frequency that is proportional to the velocity and inversely proportional to the wavelength,  $2\pi/\beta$ . The higher the velocity, the greater the voltage. Finally, if the detection electrode is a multiple of the wavelength  $2\pi/\beta$ , the voltage is zero.

If the charge density is concentrated in surface-like regions that are thin compared to other dimensions of interest, it is possible to solve Poisson’s equation with boundary conditions using a procedure that has the appearance of solving Laplace’s equation rather than Poisson’s equation. The potential is typically broken into piece-wise continuous functions, and the effect of the charge density is brought in by Gauss’ continuity condition, which is used to splice the functions at the surface occupied by the charge density. The following example illustrates this procedure. What is accomplished is a solution to Poisson’s equation in the entire region, including the charge-carrying surface.

**Example 5.6.2.** Thin Bunched Charged-Particle Beam between Conducting Plates

In microwave amplifiers and oscillators of the electron beam type, a basic problem is the evaluation of the electric field produced by a bunched electron beam. The cross-section of the beam is usually small compared with a free space wavelength of an electromagnetic wave, in which case the electroquasistatic approximation applies.

We consider a strip electron beam having a charge density that is uniform over its cross-section  $\delta$ . The beam moves with the velocity  $v$  in the  $x$  direction between two planar perfect conductors situated at  $y = \pm a$  and held at zero potential. The configuration is shown in cross-section in Fig. 5.6.3. In addition to the uniform charge density, there is a “ripple” of charge density, so that the net charge density is

$$\rho = \begin{cases} 0 & a > y > \frac{\delta}{2} \\ \rho_o + \rho_1 \cos \left[ \frac{2\pi}{\Lambda}(x - vt) \right] & \frac{\delta}{2} > y > -\frac{\delta}{2} \\ 0 & -\frac{\delta}{2} > y > -a \end{cases} \quad (15)$$

where  $\rho_o$ ,  $\rho_1$ , and  $\Lambda$  are constants. The system can be idealized to be of infinite extent in the  $x$  and  $y$  directions.

The thickness  $\delta$  of the beam is much smaller than the wavelength of the periodic charge density ripple, and much smaller than the spacing  $2a$  of the planar conductors. Thus, the beam is treated as a sheet of surface charge with a density

$$\sigma_s = \sigma_o + \sigma_1 \cos \left[ \frac{2\pi}{\Lambda}(x - vt) \right] \quad (16)$$

where  $\sigma_o = \rho_o \delta$  and  $\sigma_1 = \rho_1 \delta$ .

In regions (a) and (b), respectively, above and below the beam, the potential obeys Laplace's equation. Superscripts (a) and (b) are now used to designate variables evaluated in these regions. To guarantee that the fundamental laws are satisfied within the sheet, these potentials must satisfy the jump conditions implied by the laws of Faraday and Gauss, (5.3.4) and (5.3.5). That is, at  $y = 0$

$$\Phi^a = \Phi^b \quad (17)$$

$$-\epsilon_o \left( \frac{\partial \Phi^a}{\partial y} - \frac{\partial \Phi^b}{\partial y} \right) = \sigma_o + \sigma_1 \cos \left[ \frac{2\pi}{\Lambda} (x - vt) \right] \quad (18)$$

To complete the specification of the field in the region between the plates, boundary conditions are, at  $y = a$ ,

$$\Phi^a = 0 \quad (19)$$

and at  $y = -a$ ,

$$\Phi^b = 0 \quad (20)$$

In the respective regions, the potential is split into dc and ac parts, respectively, produced by the uniform and ripple parts of the charge density.

$$\Phi = \Phi_o + \Phi_1 \quad (21)$$

By definition,  $\Phi_o$  and  $\Phi_1$  satisfy Laplace's equation and (17), (19), and (20). The dc part,  $\Phi_o$ , satisfies (18) with only the first term on the right, while the ac part,  $\Phi_1$ , satisfies (18) with only the second term.

The dc surface charge density is independent of  $x$ , so it is natural to look for potentials that are also independent of  $x$ . From the first column in Table 5.4.1, such solutions are

$$\Phi^a = A_1 y + A_2 \quad (22)$$

$$\Phi^b = B_1 y + B_2 \quad (23)$$

The four coefficients in these expressions are determined from (17)–(20), if need be, by substitution of these expressions and formal solution for the coefficients. More attractive is the solution by inspection that recognizes that the system is symmetric with respect to  $y$ , that the uniform surface charge gives rise to uniform electric fields that are directed upward and downward in the two regions, and that the associated linear potential must be zero at the two boundaries.

$$\Phi_o^a = \frac{\sigma_o}{2\epsilon_o} (a - y) \quad (24)$$

$$\Phi_o^b = \frac{\sigma_o}{2\epsilon_o} (a + y) \quad (25)$$

Now consider the ac part of the potential. The  $x$  dependence is suggested by (18), which makes it clear that for product solutions, the  $x$  dependence of the potential must be the cosine function moving with time. Neither the sinh nor the cosh functions vanish at the boundaries, so we will have to take a linear combination of these to satisfy the boundary conditions at  $y = +a$ . This is effectively done by inspection if it is recognized that the origin of the  $y$  axis used in writing the

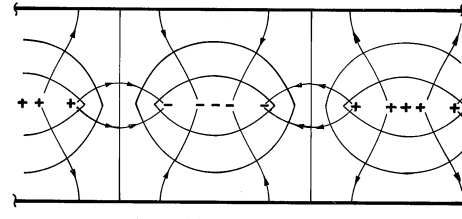


**Fig. 5.6.4** Equipotentials and field lines caused by an ac part of sheet charge in the configuration of Fig. 5.6.3.

solutions is arbitrary. The solutions to Laplace's equation that satisfy the boundary conditions, (19) and (20), are

$$\Phi_1^a = A_3 \sinh \frac{2\pi}{\Lambda}(y - a) \cos \left[ \frac{2\pi}{\Lambda}(x - vt) \right] \quad (26)$$

$$\Phi_1^b = B_3 \sinh \frac{2\pi}{\Lambda}(y + a) \cos \left[ \frac{2\pi}{\Lambda}(x - vt) \right] \quad (27)$$

These potentials must match at  $y = 0$ , as required by (17), so we might just as well have written them with the coefficients adjusted accordingly.

$$\Phi_1^a = -C \sinh \frac{2\pi}{\Lambda}(y - a) \cos \left[ \frac{2\pi}{\Lambda}(x - vt) \right] \quad (28)$$

$$\Phi_1^b = C \sinh \frac{2\pi}{\Lambda}(y + a) \cos \left[ \frac{2\pi}{\Lambda}(x - vt) \right] \quad (29)$$

The one remaining coefficient is determined by substituting these expressions into (18) (with  $\sigma_o$  omitted).

$$C = \frac{\sigma_1}{2\epsilon_o} \frac{\Lambda}{2\pi} / \cosh \left( \frac{2\pi a}{\Lambda} \right) \quad (30)$$

We have found the potential as a piece-wise continuous function. In region (a), it is the superposition of (24) and (28), while in region (b), it is (25) and (29). In both expressions,  $C$  is provided by (30).

$$\Phi^a = \frac{\sigma_o}{2\epsilon_o}(a - y) - \frac{\sigma_1}{2\epsilon_o} \frac{\Lambda}{2\pi} \frac{\sinh \left[ \frac{2\pi}{\Lambda}(y - a) \right]}{\cosh \left( \frac{2\pi a}{\Lambda} \right)} \cos \left[ \frac{2\pi}{\Lambda}(x - vt) \right] \quad (31)$$

$$\Phi^b = \frac{\sigma_o}{2\epsilon_o}(a + y) + \frac{\sigma_1}{2\epsilon_o} \frac{\Lambda}{2\pi} \frac{\sinh \left[ \frac{2\pi}{\Lambda}(y + a) \right]}{\cosh \left( \frac{2\pi a}{\Lambda} \right)} \cos \left[ \frac{2\pi}{\Lambda}(x - vt) \right] \quad (32)$$

When  $t = 0$ , the ac part of this potential distribution is as shown by Fig. 5.6.4. With increasing time, the field distribution translates to the right with the velocity  $v$ . Note that some lines of electric field intensity that originate on the beam terminate elsewhere on the beam, while others terminate on the equipotential walls. If the walls are even a wavelength away from the beam ( $a = \Lambda$ ), almost all the field lines terminate elsewhere on the beam. That is, coupling to the wall is significant only if the wavelength is on the order of or larger than  $a$ . The nature of solutions to Laplace's equation is in evidence. Two-dimensional potentials that vary rapidly in one direction must decay equally rapidly in a perpendicular direction.

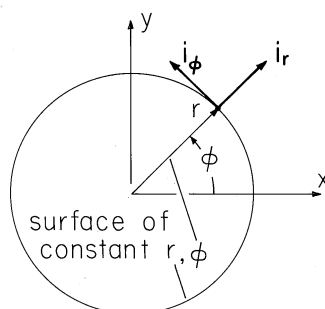


**Fig. 5.7.1** Polar coordinate system.

A comparison of the fields from the sheet beam shown in Fig. 5.6.4 and the periodic distribution of volume charge density shown in Fig. 5.6.2 is a reminder of the similarity of the two physical situations. Even though Laplace's equation applies in the subregions of the configuration considered in this section, it is really Poisson's equation that is solved "in the large," as in the previous example.

## 5.7 SOLUTIONS TO LAPLACE'S EQUATION IN POLAR COORDINATES

In electroquasistatic field problems in which the boundary conditions are specified on circular cylinders or on planes of constant  $\phi$ , it is convenient to match these conditions with solutions to Laplace's equation in polar coordinates (cylindrical coordinates with no  $z$  dependence). The approach adopted is entirely analogous to the one used in Sec. 5.4 in the case of Cartesian coordinates.

As a reminder, the polar coordinates are defined in Fig. 5.7.1. In these coordinates and with the understanding that there is no  $z$  dependence, Laplace's equation, Table I, (8), is

$$\frac{1}{r} \frac{\partial}{\partial r} \left( r \frac{\partial \Phi}{\partial r} \right) + \frac{1}{r^2} \frac{\partial^2 \Phi}{\partial \phi^2} = 0 \quad (1)$$

One difference between this equation and Laplace's equation written in Cartesian coordinates is immediately apparent: In polar coordinates, the equation contains coefficients which not only depend on the independent variable  $r$  but become singular at the origin. This singular behavior of the differential equation will affect the type of solutions we now obtain.

In order to reduce the solution of the partial differential equation to the simpler problem of solving total differential equations, we look for solutions which can be written as products of functions of  $r$  alone and of  $\phi$  alone.

$$\Phi = R(r)F(\phi) \quad (2)$$

When this assumed form of  $\phi$  is introduced into (1), and the result divided by  $\phi$  and multiplied by  $r$ , we obtain

$$\frac{r}{R} \frac{d}{dr} \left( r \frac{dR}{dr} \right) = - \frac{1}{F} \frac{d^2 F}{d\phi^2} \quad (3)$$

We find on the left-hand side of (3) a function of  $r$  alone and on the right-hand side a function of  $\phi$  alone. The two sides of the equation can balance if and only if the function of  $\phi$  and the function of  $r$  are both equal to the same constant. For this “separation constant” we introduce the symbol  $-m^2$ .

$$\frac{d^2 F}{d\phi^2} = -m^2 F \quad (4)$$

$$r \frac{d}{dr} \left( r \frac{dR}{dr} \right) = m^2 R \quad (5)$$

For  $m^2 > 0$ , the solutions to the differential equation for  $F$  are conveniently written as

$$F \sim \cos m\phi \quad \text{or} \quad \sin m\phi \quad (6)$$

Because of the space-varying coefficients, the solutions to (5) are not exponentials or linear combinations of exponentials as has so far been the case. Fortunately, the solutions are nevertheless simple. Substitution of a solution having the form  $r^n$  into (5) shows that the equation is satisfied provided that  $n = \pm m$ . Thus,

$$R \sim r^m \quad \text{or} \quad r^{-m} \quad (7)$$

In the special case of a zero separation constant, the limiting solutions are

$$F \sim \text{constant or } \phi \quad (8)$$

and

$$R \sim \text{constant or } \ln r \quad (9)$$

The product solutions shown in the first two columns of Table 5.7.1, constructed by taking all possible combinations of these solutions, are those most often used in polar coordinates. But what are the solutions if  $m^2 < 0$ ?

In Cartesian coordinates, changing the sign of the separation constant  $k^2$  amounts to interchanging the roles of the  $x$  and  $y$  coordinates. Solutions that are periodic in the  $x$  direction become exponential in character, while the exponential decay and growth in the  $y$  direction becomes periodic. Here the geometry is such that the  $r$  and  $\phi$  coordinates are not interchangeable, but the new solutions resulting from replacing  $m^2$  by  $-p^2$ , where  $p$  is a real number, essentially make the oscillating dependence radial instead of azimuthal, and the exponential dependence azimuthal rather than radial. To see this, let  $m^2 = -p^2$ , or  $m = jp$ , and the solutions given by (7) become

$$R \sim r^{jp} \quad \text{or} \quad r^{-jp} \quad (10)$$

These take a more familiar appearance if it is recognized that  $r$  can be written identically as

$$r \equiv e^{\ln r} \quad (11)$$

Introduction of this identity into (10) then gives the more familiar complex exponential, which can be split into its real and imaginary parts using Euler's formula.

$$R \sim r^{\pm jp} = e^{\pm jp \ln r} = \cos(p \ln r) \pm j \sin(p \ln r) \quad (12)$$

Thus, two independent solutions for  $R(r)$  are the cosine and sine functions of  $p \ln r$ . The  $\phi$  dependence is now either represented by  $\exp \pm p\phi$  or the hyperbolic functions that are linear combinations of these exponentials. These solutions are summarized in the right-hand column of Table 5.7.1.

In principle, the solution to a given problem can be approached by the methodical elimination of solutions from the catalogue given in Table 5.7.1. In fact, most problems are best approached by attributing to each solution some physical meaning. This makes it possible to define coordinates so that the field representation is kept as simple as possible. With that objective, consider first the solutions appearing in the first column of Table 5.7.1.

The constant potential is an obvious solution and need not be considered further. We have a solution in row two for which the potential is proportional to the angle. The equipotential lines and the field lines are illustrated in Fig. 5.7.2a. Evaluation of the field by taking the gradient of the potential in polar coordinates (the gradient operator given in Table I) shows that it becomes infinitely large as the origin is reached. The potential increases from zero to  $2\pi$  as the angle  $\phi$  is increased from zero to  $2\pi$ . If the potential is to be single valued, then we cannot allow that  $\phi$  increase further without leaving the region of validity of the solution. This observation identifies the solution with a physical field observed when two semi-infinite conducting plates are held at different potentials and the distance between the conducting plates at their junction is assumed to be negligible. In this case, shown in Fig. 5.7.2, the outside field between the plates is properly represented by a potential proportional to  $\phi$ .

With the plates separated by an angle of 90 degrees rather than 360 degrees, the potential that is proportional to  $\phi$  is seen in the corners of the configuration shown in Fig. 5.5.3. The  $m^2 = 0$  solution in the third row is familiar from Sec. 1.3, for it is the potential of a line charge. The fourth  $m^2 = 0$  solution is sketched in Fig. 5.7.3.

In order to sketch the potentials corresponding to the solutions in the second column of Table 5.7.1, the separation constant must be specified. For the time being, let us assume that  $m$  is an integer. For  $m = 1$ , the solutions  $r \cos \phi$  and  $r \sin \phi$  represent familiar potentials. Observe that the polar coordinates are related to the Cartesian ones defined in Fig. 5.7.1 by

$$\begin{aligned} r \cos \phi &= x \\ r \sin \phi &= y \end{aligned} \tag{13}$$

The fields that go with these potentials are best found by taking the gradient in Cartesian coordinates. This makes it clear that they can be used to represent uniform fields having the  $x$  and  $y$  directions, respectively. To emphasize the simplicity of these solutions, which are made complicated by the polar representation, the second function of (13) is shown in Fig. 5.7.4a.

Figure 5.7.4b shows the potential  $r^{-1} \sin \phi$ . To stay on a contour of constant potential in the first quadrant of this figure as  $\phi$  is increased toward  $\pi/2$ , it is necessary to first increase  $r$ , and then as the sine function decreases in the second quadrant, to decrease  $r$ . The potential is singular at the origin of  $r$ ; as the origin is approached from above, it is large and positive; while from below it is large and negative. Thus, the field lines emerge from the origin within  $0 < \phi < \pi$  and converge toward the origin in the lower half-plane. There must be a source at

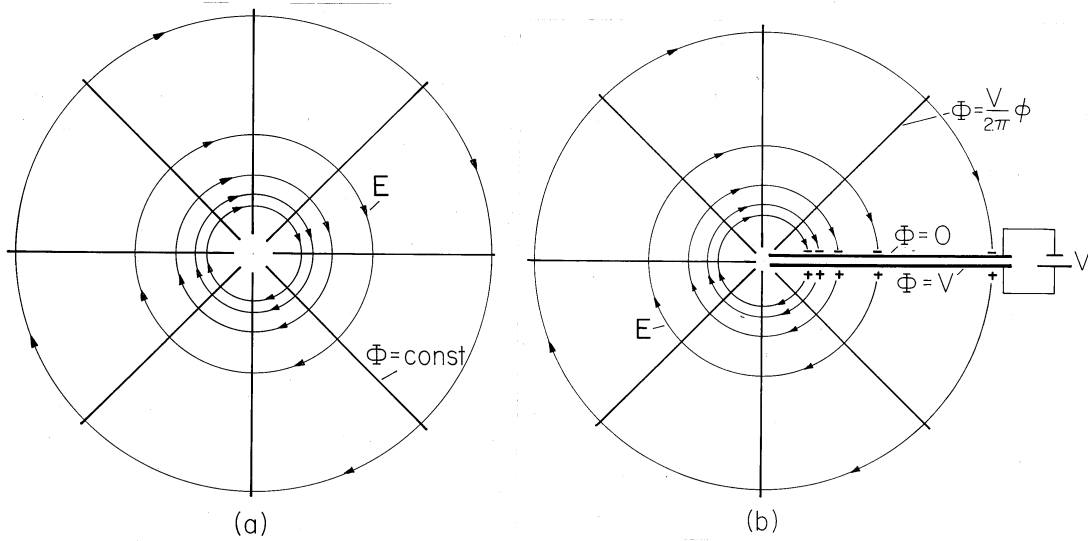


Fig. 5.7.2 Equipotentials and field lines for (a)  $\Phi = \phi$ , (b) region exterior to planar electrodes having potential difference  $V$ .

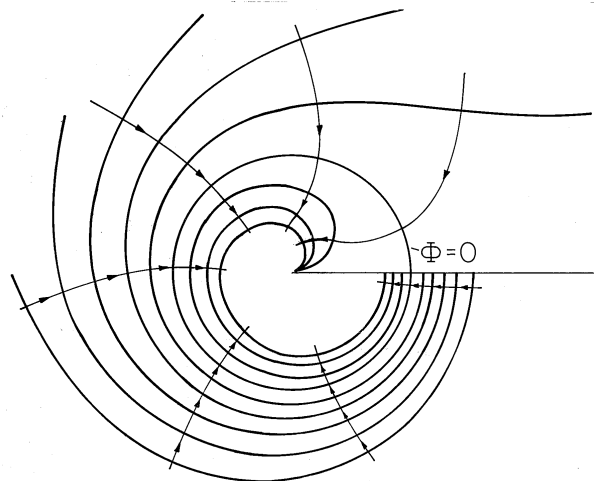
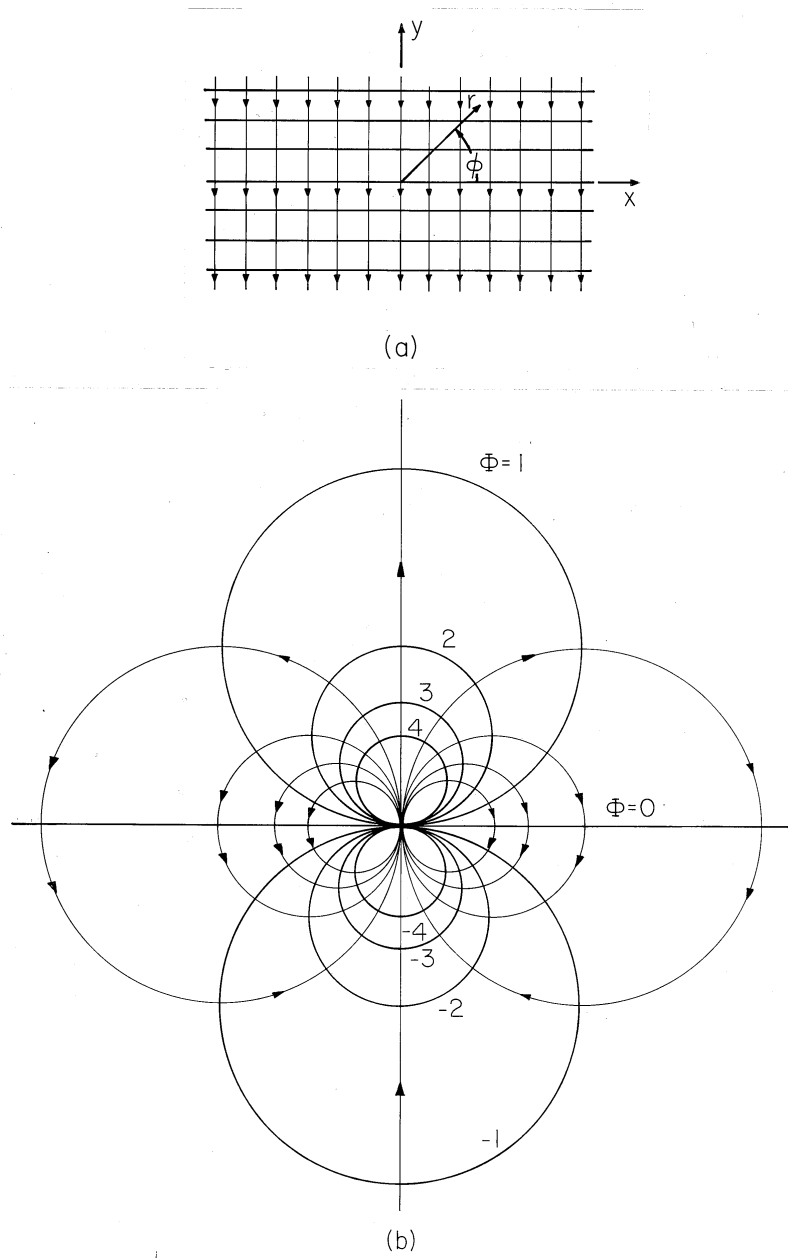


Fig. 5.7.3 Equipotentials and field lines for  $\Phi = \phi \ln(r)$ .

the origin composed of equal and opposite charges on the two sides of the plane  $r \sin \phi = 0$ . The source, which is uniform and of infinite extent in the  $z$  direction, is a line dipole.

This conclusion is confirmed by direct evaluation of the potential produced by two line charges, the charge  $-\lambda_l$  situated at the origin, the charge  $+\lambda_l$  at a very small distance away from the origin at  $r = d$ ,  $\phi = \pi/2$ . The potential follows from



**Fig. 5.7.4** Equipotentials and field lines for (a)  $\Phi = r \sin(\phi)$ , (b)  $\Phi = r^{-1} \sin(\phi)$ .



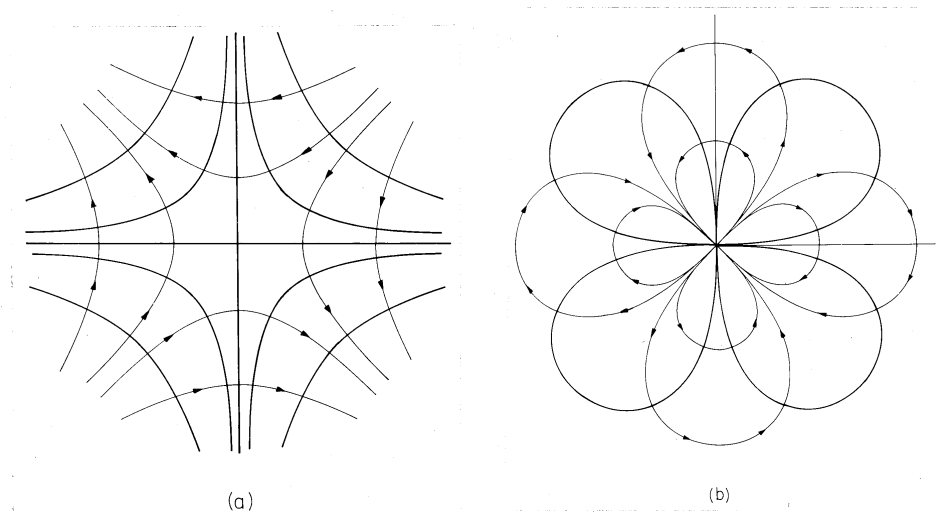


**Fig. 5.7.5** Equipotentials and field lines for (a)  $\Phi = r^2 \sin(2\phi)$ , (b)  $\Phi = r^{-2} \sin(2\phi)$ .

steps paralleling those used for the three-dimensional dipole in Sec. 4.4.

$$\Phi = \lim_{\substack{d \rightarrow 0 \\ \lambda_l \rightarrow \infty}} \left[ -\frac{\lambda_l}{2\pi\epsilon_o} \ln(r - d \sin \phi) + \frac{\lambda_l}{2\pi\epsilon_o} \ln r \right] = \frac{p_\lambda}{2\pi\epsilon_o} \frac{\sin \phi}{r} \quad (14)$$

The spatial dependence of the potential is indeed  $\sin \phi/r$ . In an analogy with the three-dimensional dipole of Sec. 4.4,  $p_\lambda \equiv \lambda_l d$  is defined as the line dipole moment. In Example 4.6.3, it is shown that the equipotentials for parallel line charges are circular cylinders. Because this result is independent of spacing between the line charges, it is no surprise that the equipotentials of Fig. 5.7.4b are circular.

In summary, the  $m = 1$  solutions can be thought of as the fields of dipoles at infinity and at the origin. For the sine dependencies, the dipoles are  $y$  directed, while for the cosine dependencies they are  $x$  directed.

The solution of Fig. 5.7.5a,  $\phi \propto r^2 \sin 2\phi$ , has been met before in Cartesian coordinates. Either from a comparison of the equipotential plots or by direct transformation of the Cartesian coordinates into polar coordinates, the potential is recognized as  $xy$ .

The  $m = 2$  solution that is singular at the origin is shown in Fig. 5.7.5b. Field lines emerge from the origin and return to it twice as  $\phi$  ranges from 0 to  $2\pi$ . This observation identifies four line charges of equal magnitude, alternating in sign as the source of the field. Thus, the  $m = 2$  solutions can be regarded as those of quadrupoles at infinity and at the origin.

It is perhaps a bit surprising that we have obtained from Laplace's equation solutions that are singular at the origin and hence associated with sources at the origin. The singularity of one of the two independent solutions to (5) can be traced to the singularity in the coefficients of this differential equation.

From the foregoing, it is seen that increasing  $m$  introduces a more rapid variation of the field with respect to the angular coordinate. In problems where

TABLE 5.7.1		
SOLUTIONS TO LAPLACE'S EQUATION		
IN POLAR COORDINATES		
$m = 0$	$m^2 \geq 0$	$m^2 \leq 0 (m \rightarrow jp)$
Constant		$\cos[p \ln(r)] \cosh p\phi$
$\phi$		$\cos[p \ln(r)] \sinh p\phi$
$\ln r$		$\sin [p \ln(r)] \cosh p\phi$
$\phi \ln r$		$\sin [p \ln(r)] \sinh p\phi$
	$r^m \cos m\phi$	$\cos [p \ln(r)] e^{p\phi}$
	$r^m \sin m\phi$	$\cos [p \ln(r)] e^{-p\phi}$
	$r^{-m} \cos m\phi$	$\sin [p \ln(r)] e^{p\phi}$
	$r^{-m} \sin m\phi$	$\sin [p \ln(r)] e^{-p\phi}$

the region of interest includes all values of  $\phi$ ,  $m$  must be an integer to make the field return to the same value after one revolution. But,  $m$  does not have to be an integer. If the region of interest is pie shaped,  $m$  can be selected so that the potential passes through one cycle over an arbitrary interval of  $\phi$ . For example, the periodicity angle can be made  $\phi_o$  by making  $m\phi_o = n\pi$  or  $m = n\pi/\phi_o$ , where  $n$  can have any integer value.

The solutions for  $m^2 < 0$ , the right-hand column of Table 5.7.1, are illustrated in Fig. 5.7.6 using as an example essentially the fourth solution. Note that the radial phase has been shifted by subtracting  $p \ln(b)$  from the argument of the sine. Thus, the potential shown is

$$\Phi = \sin [p \ln(r/b)] \sinh p\phi \tag{15}$$

and it automatically passes through zero at the radius  $r = b$ . The distances between radii of zero potential are not equal. Nevertheless, the potential distribution is qualitatively similar to that in Cartesian coordinates shown in Fig. 5.4.2. The exponential dependence is azimuthal; that direction is thus analogous to  $y$  in Fig. 5.4.2. In essence, the potentials for  $m^2 < 0$  are similar to those in Cartesian coordinates but wrapped around the  $z$  axis.

### 5.8 EXAMPLES IN POLAR COORDINATES

With the objective of attaching physical insight to the polar coordinate solutions to Laplace's equation, two types of examples are of interest. First are certain classic

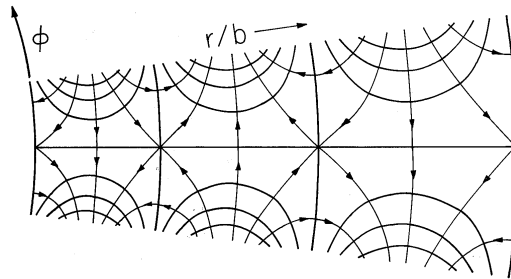


**Fig. 5.7.6** Equipotentials and field lines representative of solutions in right-hand column of Table 5.7.1. Potential shown is given by (15).

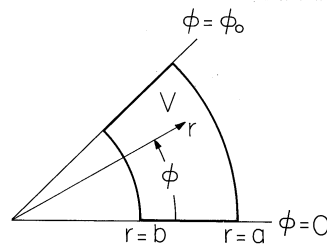


**Fig. 5.8.1** Natural boundaries in polar coordinates enclose region  $V$ .

problems that have simple solutions. Second are examples that require the generally applicable modal approach that makes it possible to satisfy arbitrary boundary conditions.

The equipotential cylinder in a uniform applied electric field considered in the first example is in the first category. While an important addition to our resource of case studies, the example is also of practical value because it allows estimates to be made in complex engineering systems, perhaps of the degree to which an applied field will tend to concentrate on a cylindrical object.

In the most general problem in the second category, arbitrary potentials are imposed on the polar coordinate boundaries enclosing a region  $V$ , as shown in Fig. 5.8.1. The potential is the superposition of four solutions, each meeting the potential constraint on one of the boundaries while being zero on the other three. In Cartesian coordinates, the approach used to find one of these four solutions, the modal approach of Sec. 5.5, applies directly to the other three. That is, in writing the solutions, the roles of  $x$  and  $y$  can be interchanged. On the other hand, in polar coordinates the set of solutions needed to represent a potential imposed on the boundaries at  $r = a$  or  $r = b$  is different from that appropriate for potential constraints on the boundaries at  $\phi = 0$  or  $\phi = \phi_0$ . Examples 5.8.2 and 5.8.3 illustrate the two types of solutions needed to determine the fields in the most general case. In the second of these, the potential is expanded in a set of orthogonal functions that are not sines or cosines. This gives the opportunity to form an appreciation for an orthogonality property of the product solutions to Laplace's equation that prevails in many other coordinate systems.

**Simple Solutions.** The example considered now is the first in a series of “cylinder” case studies built on the same  $m = 1$  solutions. In the next chapter, the cylinder will become a polarizable dielectric. In Chap. 7, it will have finite conductivity and provide the basis for establishing just how “perfect” a conductor must be to justify the equipotential model used here. In Chaps. 8–10, the field will be magnetic and the cylinder first perfectly conducting, then magnetizable, and finally a shell of finite conductivity. Because of the simplicity of the dipole solutions used in this series of examples, in each case it is possible to focus on the physics without becoming distracted by mathematical details.

**Example 5.8.1.** Equipotential Cylinder in a Uniform Electric Field

A uniform electric field  $E_a$  is applied in a direction perpendicular to the axis of a (perfectly) conducting cylinder. Thus, the surface of the conductor, which is at  $r = R$ , is an equipotential. The objective is to determine the field distribution as modified by the presence of the cylinder.

Because the boundary condition is stated on a circular cylindrical surface, it is natural to use polar coordinates. The field excitation comes from “infinity,” where the field is known to be uniform, of magnitude  $E_a$ , and  $x$  directed. Because our solution must approach this uniform field far from the cylinder, it is important to recognize at the outset that its potential, which in Cartesian coordinates is  $-E_a x$ , is

$$\Phi(r \rightarrow \infty) \rightarrow -E_a r \cos \phi \quad (1)$$

To this must be added the potential produced by the charges induced on the surface of the conductor so that the surface is maintained an equipotential. Because the solutions have to hold over the entire range  $0 < \phi < 2\pi$ , only integer values of the separation constant  $m$  are allowed, i.e., only solutions that are periodic in  $\phi$ . If we are to add a function to (1) that makes the potential zero at  $r = R$ , it must cancel the value given by (1) at each point on the surface of the cylinder. There are two solutions in Table 5.7.1 that have the same  $\cos \phi$  dependence as (1). We pick the  $1/r$  dependence because it decays to zero as  $r \rightarrow \infty$  and hence does not disturb the potential at infinity already given by (1). With  $A$  an arbitrary coefficient, the solution is therefore

$$\Phi = -E_a r \cos \phi + \frac{A}{r} \cos \phi \quad (2)$$

Because  $\Phi = 0$  at  $r = R$ , evaluation of this expression shows that the boundary condition is satisfied at every angle  $\phi$  if

$$A = E_a R^2 \quad (3)$$

and the potential is therefore

$$\Phi = -E_a R \left[ \frac{r}{R} - \frac{R}{r} \right] \cos \phi \quad (4)$$

The equipotentials given by this expression are shown in Fig. 5.8.2. Note that the  $x = 0$  plane has been taken as having zero potential by omitting an additive constant in (1). The field lines shown in this figure follow from taking the gradient of (4).

$$\mathbf{E} = \mathbf{i}_r E_a \left[ 1 + \left( \frac{R}{r} \right)^2 \right] \cos \phi - \mathbf{i}_\phi E_a \left[ 1 - \left( \frac{R}{r} \right)^2 \right] \sin \phi \quad (5)$$

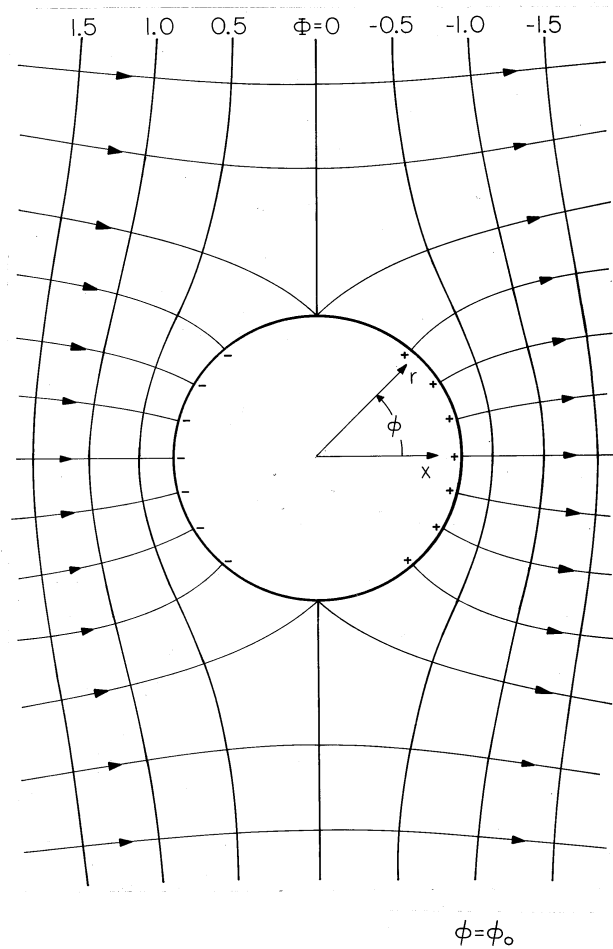


**Fig. 5.8.2** Equipotentials and field lines for perfectly conducting cylinder in initially uniform electric field.

Field lines tend to concentrate on the surface where  $\phi = 0$  and  $\phi = \pi$ . At these locations, the field is maximum and twice the applied field. Now that the boundary value problem has been solved, the surface charge on the cylindrical conductor follows from Gauss' jump condition, (5.3.2), and the fact that there is no field inside the cylinder.

$$\sigma_s = \mathbf{n} \cdot \epsilon_o \mathbf{E} = \epsilon_o E_r \Big|_{r=R} = 2\epsilon_o E_a \cos \phi \tag{6}$$

In retrospect, the boundary condition on the circular cylindrical surface has been satisfied by adding to the uniform potential that of an  $x$  directed line dipole. Its moment is that necessary to create a field that cancels the tangential field on the surface caused by the imposed field.

**Azimuthal Modes.** The preceding example considered a situation in which Laplace's equation is obeyed in the entire range  $0 < \phi < 2\pi$ . The next two examples

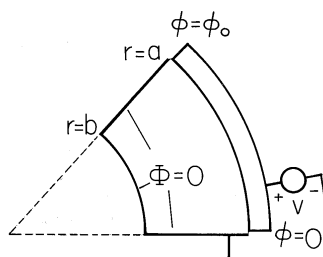


**Fig. 5.8.3** Region of interest with zero potential boundaries at  $\phi = 0$ ,  $\Phi = \phi_o$ , and  $r = b$  and electrode at  $r = a$  having potential  $v$ .

illustrate how the polar coordinate solutions are adapted to meeting conditions on polar coordinate boundaries that have arbitrary locations as pictured in Fig. 5.8.1.

**Example 5.8.2.** Modal Analysis in  $\phi$ : Fields in and around Corners

The configuration shown in Fig. 5.8.3, where the potential is zero on the walls of the region  $V$  at  $r = b$  and at  $\phi = 0$  and  $\phi = \phi_o$ , but is  $v$  on a curved electrode at  $r = a$ , is the polar coordinate analogue of that considered in Sec. 5.5. What solutions from Table 5.7.1 are pertinent? The region within which Laplace's equation is to be obeyed does not occupy a full circle, and hence there is no requirement that the potential be a single-valued function of  $\phi$ . The separation constant  $m$  can assume noninteger values.

We shall attempt to satisfy the boundary conditions on the three zero-potential boundaries using individual solutions from Table 5.7.1. Because the potential is zero at  $\phi = 0$ , the cosine and  $\ln(r)$  terms are eliminated. The requirement that the potential also be zero at  $\phi = \phi_o$  eliminates the functions  $\phi$  and  $\phi \ln(r)$ . Moreover, the fact that the remaining sine functions must be zero at  $\phi = \phi_o$  tells us that  $m\phi_o = n\pi$ . Solutions in the last column are not appropriate because they do not pass through zero more than once as a function of  $\phi$ . Thus, we are led to the two solutions in the second column that are proportional to  $\sin(n\pi\phi/\phi_o)$ .

$$\Phi = \sum_{n=1}^{\infty} \left[ A_n \left(\frac{r}{b}\right)^{n\pi/\phi_o} + B_n \left(\frac{r}{b}\right)^{-n\pi/\phi_o} \right] \sin\left(\frac{n\pi\phi}{\phi_o}\right) \quad (7)$$

In writing these solutions, the  $r$ 's have been normalized to  $b$ , because it is then clear by inspection how the coefficients  $A_n$  and  $B_n$  are related to make the potential zero at  $r = b$ ,  $A_n = -B_n$ .

$$\Phi = \sum_{n=1}^{\infty} A_n \left[ \left(\frac{r}{b}\right)^{n\pi/\phi_o} - \left(\frac{r}{b}\right)^{-n\pi/\phi_o} \right] \sin\left(\frac{n\pi\phi}{\phi_o}\right) \quad (8)$$

Each term in this infinite series satisfies the conditions on the three boundaries that are constrained to zero potential. All of the terms are now used to meet the condition at the "last" boundary, where  $r = a$ . There we must represent a potential which jumps abruptly from zero to  $v$  at  $\phi = 0$ , stays at the same  $v$  up to  $\phi = \phi_o$ , and then jumps abruptly from  $v$  back to zero. The determination of the coefficients in (8) that make the series of sine functions meet this boundary condition is the same as for (5.5.4) in the Cartesian analogue considered in Sec. 5.5. The parameter  $n\pi(x/a)$

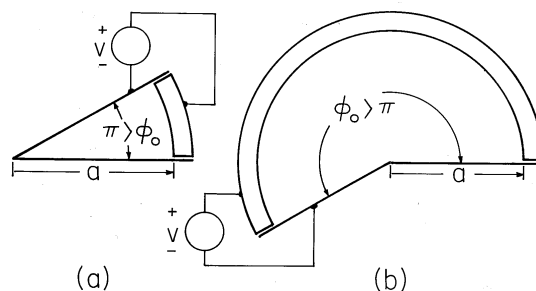


**Fig. 5.8.4** Pie-shaped region with zero potential boundaries at  $\phi = 0$  and  $\phi = \phi_o$  and electrode having potential  $v$  at  $r = a$ . (a) With included angle less than 180 degrees, fields are shielded from region near origin. (b) With angle greater than 180 degrees, fields tend to concentrate at origin.

of Sec. 5.5 is now to be identified with  $n\pi(\phi/\phi_o)$ . With the potential given by (8) evaluated at  $r = a$ , the coefficients must be as in (5.5.17) and (5.5.18). Thus, to meet the “last” boundary condition, (8) becomes the desired potential distribution.

$$\Phi = \sum_{\substack{n=1 \\ \text{odd}}}^{\infty} \frac{4v}{n\pi} \frac{\left[ \left(\frac{r}{b}\right)^{n\pi/\phi_o} - \left(\frac{r}{b}\right)^{-n\pi/\phi_o} \right]}{\left[ \left(\frac{a}{b}\right)^{n\pi/\phi_o} - \left(\frac{a}{b}\right)^{-n\pi/\phi_o} \right]} \sin\left(\frac{n\pi}{\phi_o}\phi\right) \quad (9)$$

The distribution of potential and field intensity implied by this result is much like that for the region of rectangular cross-section depicted in Fig. 5.5.3. See Fig. 5.8.3.

In the limit where  $b \rightarrow 0$ , the potential given by (9) becomes

$$\Phi = \sum_{\substack{n=1 \\ \text{odd}}}^{\infty} \frac{4v}{n\pi} \left(\frac{r}{a}\right)^{n\pi/\phi_o} \sin\frac{n\pi}{\phi_o}\phi \quad (10)$$

and describes the configurations shown in Fig. 5.8.4. Although the wedge-shaped region is a reasonable “distortion” of its Cartesian analogue, the field in a region with an outside corner ( $\pi/\phi_o < 1$ ) is also represented by (10). As long as the leading term has the exponent  $\pi/\phi_o > 1$ , the leading term in the gradient [with the exponent  $(\pi/\phi_o) - 1$ ] approaches zero at the origin. This means that the field in a wedge with  $\phi_o < \pi$  approaches zero at its apex. However, if  $\pi/\phi_o < 1$ , which is true for  $\pi < \phi_o < 2\pi$  as illustrated in Fig. 5.8.4b, the leading term in the gradient of  $\Phi$  has the exponent  $(\pi/\phi_o) - 1 < 0$ , and hence the field approaches infinity as  $r \rightarrow 0$ . We conclude that the field in the neighborhood of a sharp edge is infinite. This observation teaches a lesson for the design of conductor shapes so as to avoid electrical breakdown. Avoid sharp edges!

**Radial Modes.** The modes illustrated so far possessed sinusoidal  $\phi$  dependencies, and hence their superposition has taken the form of a Fourier series. To satisfy boundary conditions imposed on constant  $\phi$  planes, it is again necessary to have an infinite set of solutions to Laplace’s equation. These illustrate how the

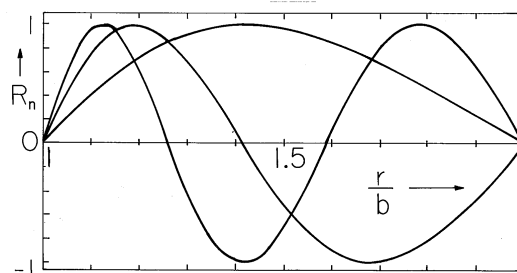


**Fig. 5.8.5** Radial distribution of first three modes given by (13) for  $a/b = 2$ . The  $n = 3$  mode is the radial dependence for the potential shown in Fig. 5.7.6.

product solutions to Laplace's equation can be used to provide orthogonal modes that are not Fourier series.

To satisfy zero potential boundary conditions at  $r = b$  and  $r = a$ , it is necessary that the function pass through zero at least twice. This makes it clear that the solutions must be chosen from the last column in Table 5.7.1. The functions that are proportional to the sine and cosine functions can just as well be proportional to the sine function shifted in phase (a linear combination of the sine and cosine). This phase shift is adjusted to make the function zero where  $r = b$ , so that the radial dependence is expressed as

$$R(r) = \sin[p \ln(r) - p \ln(b)] = \sin[p \ln(r/b)] \quad (11)$$

and the function made to be zero at  $r = a$  by setting

$$p \ln(a/b) = n\pi \Rightarrow p = \frac{n\pi}{\ln(a/b)} \quad (12)$$

where  $n$  is an integer.

The solutions that have now been defined can be superimposed to form a series analogous to the Fourier series.

$$S(r) = \sum_{n=1}^{\infty} S_n R_n(r); \quad R_n \equiv \sin \left[ n\pi \frac{\ln(r/b)}{\ln(a/b)} \right] \quad (13)$$

For  $a/b = 2$ , the first three terms in the series are illustrated in Fig. 5.8.5. They have similarity to sinusoids but reflect the polar geometry by having peaks and zero crossings skewed toward low values of  $r$ .

With a weighting function  $g(r) = r^{-1}$ , these modes are orthogonal in the sense that

$$\int_b^a \frac{1}{r} \sin \left[ n\pi \frac{\ln(r/b)}{\ln(a/b)} \right] \sin \left[ m\pi \frac{\ln(r/b)}{\ln(a/b)} \right] dr = \begin{cases} \frac{1}{2} \ln(a/b), & m = n \\ 0, & m \neq n \end{cases} \quad (14)$$

It can be shown from the differential equation defining  $R(r)$ , (5.7.5), and the boundary conditions, that the integration gives zero if the integration is over



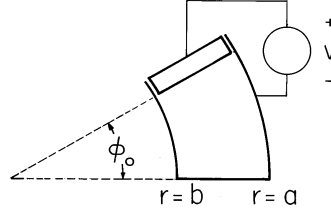


**Fig. 5.8.6** Region with zero potential boundaries at  $r = a$ ,  $r = b$ , and  $\phi = 0$ . Electrode at  $\phi = \phi_o$  has potential  $v$ .

the product of different modes. The proof is analogous to that given in Cartesian coordinates in Sec. 5.5.

Consider now an example in which these modes are used to satisfy a specific boundary condition.

**Example 5.8.3.** Modal Analysis in  $r$

The region of interest is of the same shape as in the previous example. However, as shown in Fig. 5.8.6, the zero potential boundary conditions are at  $r = a$  and  $r = b$  and at  $\phi = 0$ . The “last” boundary is now at  $\phi = \phi_o$ , where an electrode connected to a voltage source imposes a uniform potential  $v$ .

The radial boundary conditions are satisfied by using the functions described by (13) for the radial dependence. Because the potential is zero where  $\phi = 0$ , it is then convenient to use the hyperbolic sine to represent the  $\phi$  dependence. Thus, from the solutions in the last column of Table 5.7.1, we take a linear combination of the second and fourth.

$$\Phi = \sum_{n=1}^{\infty} A_n \sin \left[ n\pi \frac{\ln(r/b)}{\ln(a/b)} \right] \sinh \left[ \frac{n\pi}{\ln(a/b)} \phi \right] \quad (15)$$

Using an approach that is analogous to that for evaluating the Fourier coefficients in Sec. 5.5, we now use (15) on the “last” boundary, where  $\phi = \phi_o$  and  $\Phi = v$ , multiply both sides by the mode  $R_m$  defined with (13) and by the weighting factor  $1/r$ , and integrate over the radial span of the region.

$$\int_b^a \frac{1}{r} \Phi(r, \phi_o) \sin \left[ m\pi \frac{\ln(r/b)}{\ln(a/b)} \right] dr = \sum_{n=1}^{\infty} \int_b^a \frac{A_n}{r} \sinh \left[ \frac{n\pi}{\ln(a/b)} \phi_o \right] \cdot \sin \left[ n\pi \frac{\ln(r/b)}{\ln(a/b)} \right] \sin \left[ m\pi \frac{\ln(r/b)}{\ln(a/b)} \right] dr \quad (16)$$

Out of the infinite series on the right, the orthogonality condition, (14), picks only the  $m$ -th term. Thus, the equation can be solved for  $A_m$  and  $m \rightarrow n$ . With the substitution  $u = m\pi \ln(r/b)/\ln(a/b)$ , the integrals can be carried out in closed form.

$$A_n = \begin{cases} \frac{4v}{n\pi \sinh \left[ \frac{n\pi}{\ln(a/b)} \phi_o \right]}, & n \text{ odd} \\ 0, & n \text{ even} \end{cases} \quad (17)$$

A picture of the potential and field intensity distributions represented by (15) and its negative gradient is visualized by “bending” the rectangular region shown by Fig. 5.5.3 into the curved region of Fig. 5.8.6. The role of  $y$  is now played by  $\phi$ .

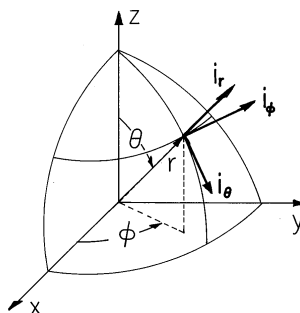


Fig. 5.9.1 Spherical coordinate system.

### 5.9 THREE SOLUTIONS TO LAPLACE'S EQUATION IN SPHERICAL COORDINATES

The method employed to solve Laplace's equation in Cartesian coordinates can be repeated to solve the same equation in the spherical coordinates of Fig. 5.9.1. We have so far considered solutions that depend on only two independent variables. In spherical coordinates, these are commonly  $r$  and  $\theta$ . These two-dimensional solutions therefore satisfy boundary conditions on spheres and cones.

Rather than embark on an exploration of product solutions in spherical coordinates, attention is directed in this section to three such solutions to Laplace's equation that are already familiar and that are remarkably useful. These will be used to explore physical processes ranging from polarization and charge relaxation dynamics to the induction of magnetization and eddy currents.

Under the assumption that there is no  $\phi$  dependence, Laplace's equation in spherical coordinates is (Table I)

$$\frac{1}{r^2} \frac{\partial}{\partial r} \left( r^2 \frac{\partial \Phi}{\partial r} \right) + \frac{1}{r^2 \sin \theta} \frac{\partial}{\partial \theta} \left( \sin \theta \frac{\partial \Phi}{\partial \theta} \right) = 0 \quad (1)$$

The first of the three solutions to this equation is independent of  $\theta$  and is the potential of a point charge.

$$\Phi \sim \frac{1}{r} \quad (2)$$

If there is any doubt, substitution shows that Laplace's equation is indeed satisfied. Of course, it is not satisfied at the origin where the point charge is located.

Another of the solutions found before is the three-dimensional dipole, (4.4.10).

$$\Phi \sim \frac{\cos \theta}{r^2} \quad (3)$$

This solution factors into a function of  $r$  alone and of  $\theta$  alone, and hence would have to turn up in developing the product solutions to Laplace's equation in spherical coordinates. Substitution shows that it too is a solution of (1).

The third solution represents a uniform  $z$ -directed electric field in spherical coordinates. Such a field has a potential that is linear in  $z$ , and in spherical coordinates,  $z = r \cos \theta$ . Thus, the potential is

$$\Phi \sim r \cos \theta \quad (4)$$

These last two solutions, for the three-dimensional dipole at the origin and a field due to  $\pm$  charges at  $z \rightarrow \pm\infty$ , are similar to those for dipoles in two dimensions, the  $m = 1$  solutions that are proportional to  $\cos \phi$  from the second column of Table 5.7.1. However, note that the two-dimensional dipole potential varies as  $r^{-1}$ , while the three dimensional dipole potential has an  $r^{-2}$  dependence. Also note that whereas the polar coordinate dipole can have an arbitrary orientation (can be a sine as well as a cosine function of  $\phi$ , or any linear combination of these), the three-dimensional dipole is  $z$  directed. That is, do not replace the cosine function in (3) by a sine function and expect that the potential will satisfy Laplace's equation in spherical coordinates.

**Example 5.9.1.** Equipotential Sphere in a Uniform Electrical Field

Consider a raindrop in an electric field. If in the absence of the drop, that field is uniform over many drop radii  $R$ , the field in the vicinity of the drop can be computed by taking the field as being uniform "far from the sphere." The field is  $z$  directed and has a magnitude  $E_a$ . Thus, on the scale of the drop, the potential must approach that of the uniform field (4) as  $r \rightarrow \infty$ .

$$\Phi(r \rightarrow \infty) \rightarrow -E_a r \cos \theta \quad (5)$$

We will see in Chap. 7 that it takes only microseconds for a water drop in air to become an equipotential. The condition that the potential be zero at  $r = R$  and yet approach the potential of (5) as  $r \rightarrow \infty$  is met by adding to (5) the potential of a dipole at the origin, an adjustable coefficient times (3). By writing the  $r$  dependencies normalized to the drop radius  $R$ , it is possible to see directly what this coefficient must be. That is, the proposed solution is

$$\Phi = -E_a R \cos \theta \left[ \frac{r}{R} + A \left( \frac{R}{r} \right)^2 \right] \quad (6)$$

and it is clear that to make this function zero at  $r = R$ ,  $A = -1$ .

$$\Phi = -E_a R \cos \theta \left[ \frac{r}{R} - \left( \frac{R}{r} \right)^2 \right] \quad (7)$$

Note that even though the configuration of a perfectly conducting rod in a uniform transverse electric field (as considered in Example 5.8.1) is very different from the perfectly conducting sphere in a uniform electric field, the potentials are deduced from very similar arguments, and indeed the potentials appear similar. In cross-section, the distribution of potential and field intensity is similar to that for the cylinder shown in Fig. 5.8.2. Of course, their appearance in three-dimensional space is very different. For the polar coordinate configuration, the equipotentials shown are the cross-sections of cylinders, while for the spherical drop they are cross-sections of surfaces of revolution. In both cases, the potential acquired (by the sphere or the rod) is that of the symmetry plane normal to the applied field.

The surface charge on the spherical surface follows from (7).

$$\sigma_s = -\epsilon_o \mathbf{n} \cdot \nabla \Phi \Big|_{r=R} = \epsilon_o E_r \Big|_{r=R} = 3\epsilon_o E_a \cos \theta \quad (8)$$

Thus, for  $E_a > 0$ , the north pole is capped by positive surface charge while the south pole has negative charge. Although we think of the second solution in (7) as being

due to a fictitious dipole located at the sphere's center, it actually represents the field of these surface charges. By contrast with the rod, where the maximum field is twice the uniform field, it follows from (8) that the field intensifies by a factor of three at the poles of the sphere.

In making practical use of the solution found here, the "uniform field at infinity  $E_a$ " is that of a field that is slowly varying over dimensions on the order of the drop radius  $R$ . To demonstrate this idea in specific terms, suppose that the imposed field is due to a distant point charge. This is the situation considered in Example 4.6.4, where the field produced by a point charge and a conducting sphere is considered. If the point charge is very far away from the sphere, its field at the position of the sphere is essentially uniform over the region occupied by the sphere. (To relate the directions of the fields in Example 4.6.4 to the present case, mount the  $\theta = 0$  axis from the center of the sphere pointing towards the point charge. Also, to make the field in the vicinity of the sphere positive, make the point charge negative,  $q \rightarrow -q$ .)

At the sphere center, the magnitude of the field intensity due to the point charge is

$$E_a = \frac{q}{4\pi\epsilon_o X^2} \quad (9)$$

The magnitude of the image charge, given by (4.6.34), is

$$Q_1 = \frac{|q|R}{X} \quad (10)$$

and it is positioned at the distance  $D = R^2/X$  from the center of the sphere. If the sphere is to be charge free, a charge of strength  $-Q_1$  has to be mounted at its center. If  $X$  is very large compared to  $R$ , the distance  $D$  becomes small enough so that this charge and the charge given by (10) form a dipole of strength

$$p = \frac{Q_1 R^2}{X} = \frac{|q|R^3}{X^2} \quad (11)$$

The potential resulting from this dipole moment is given by (4.4.10), with  $p$  evaluated using this moment. With the aid of (9), the dipole field induced by the point charge is recognized as

$$\Phi = \frac{p}{4\pi\epsilon_o r^2} \cos\theta = E_a \frac{R^3}{r^2} \cos\theta \quad (12)$$

As witnessed by (7), this potential is identical to the one we have found necessary to add to the potential of the uniform field in order to match the boundary conditions on the sphere.

Of the three spherical coordinate solutions to Laplace's equation given in this section, only two were required in the previous example. The next makes use of all three.

**Example 5.9.2.** Charged Equipotential Sphere in a Uniform Electric Field

Suppose that the highly conducting sphere from Example 5.9.1 carries a net charge  $q$  while immersed in a uniform applied electric field  $E_a$ . Thunderstorm electrification is evidence that raindrops are often charged, and  $E_a$  could be the field they generate collectively.

In the absence of this net charge, the potential is given by (7). On the boundary at  $r = R$ , this potential remains uniform if we add the potential of a point charge at the origin of magnitude  $q$ .

$$\Phi = -E_a R \cos \theta \left[ \frac{r}{R} - \left( \frac{R}{r} \right)^2 \right] + \frac{q}{4\pi\epsilon_o r} \quad (13)$$

The surface potential has been raised from zero to  $q/4\pi\epsilon_o R$ , but this potential is independent of  $\phi$  and so the tangential electric field remains zero.

The point charge is, of course, fictitious. The actual charge is distributed over the surface and is found from (13) to be

$$\sigma_s = -\epsilon_o \left. \frac{\partial \Phi}{\partial r} \right|_{r=R} = 3\epsilon_o E_a \left( \cos \theta + \frac{q}{q_c} \right); \quad q_c \equiv 12\pi\epsilon_o E_a R^2 \quad (14)$$

The surface charge density switches sign when the term in parentheses vanishes, when  $q/q_c < 1$  and

$$-\cos \theta_c = \frac{q}{q_c} \quad (15)$$

Figure 5.9.2a is a graphical solution of this equation. For  $E_a$  and  $q$  positive, the positive surface charge capping the sphere extends into the southern hemisphere. The potential and electric field distributions implied by (13) are illustrated in Fig. 5.9.2b. If  $q$  exceeds  $q_c \equiv 12\pi\epsilon_o E_a R^2$ , the entire surface of the sphere is covered with positive surface charge density and  $\mathbf{E}$  is directed outward over the entire surface.

## 5.10 THREE-DIMENSIONAL SOLUTIONS TO LAPLACE'S EQUATION

Natural boundaries enclosing volumes in which Poisson's equation is to be satisfied are shown in Fig. 5.10.1 for the three standard coordinate systems. In general, the distribution of potential is desired within the volume with an arbitrary potential distribution on the bounding surfaces.

Considered first in this section is the extension of the Cartesian coordinate two-dimensional product solutions and modal expansions introduced in Secs. 5.4 and 5.5 to three dimensions. Given an arbitrary potential distribution over one of the six surfaces of the box shown in Fig. 5.10.1, and given that the other five surfaces are at zero potential, what is the solution to Laplace's equation within? If need be, a superposition of six such solutions can be used to satisfy arbitrary conditions on all six boundaries.

To use the same modal approach in configurations where the boundaries are natural to other than Cartesian coordinate systems, for example the cylindrical and spherical ones shown in Fig. 5.10.1, essentially the same extension of the basic ideas already illustrated is used. However, the product solutions involve less familiar functions. For those who understand the two-dimensional solutions, how they are used to meet arbitrary boundary conditions and how they are extended to three-dimensional Cartesian coordinate configurations, the literature cited in this section should provide ready access to what is needed to exploit solutions in new coordinate systems. In addition to the three standard coordinate systems, there are many

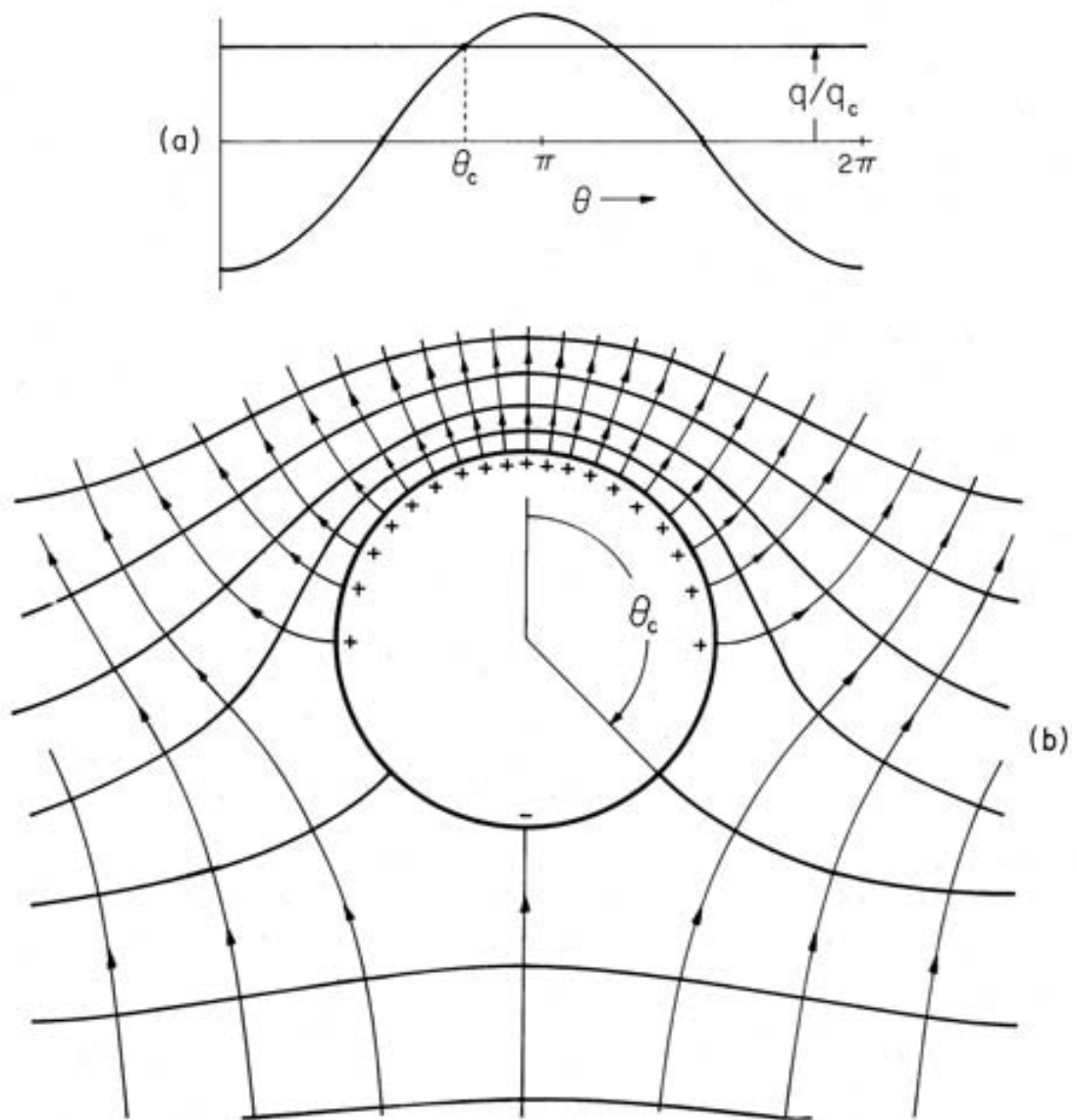


**Fig. 5.9.2** (a) Graphical solution of (15) for angle  $\theta_c$  at which electric field switches from being outward to being inward directed on surface of sphere. (b) Equipotentials and field lines for perfectly conducting sphere having net charge  $q$  in an initially uniform electric field.

others in which Laplace's equation admits product solutions. The latter part of this section is intended as an introduction to these coordinate systems and associated product solutions.

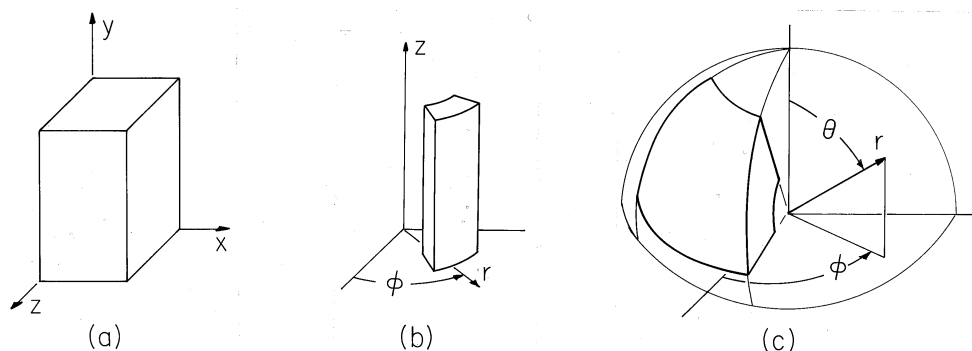


**Fig. 5.10.1** Volumes defined by natural boundaries in (a) Cartesian, (b) cylindrical, and (c) spherical coordinates.

**Cartesian Coordinate Product Solutions.** In three-dimensions, Laplace's equation is

$$\frac{\partial^2 \Phi}{\partial x^2} + \frac{\partial^2 \Phi}{\partial y^2} + \frac{\partial^2 \Phi}{\partial z^2} = 0 \quad (1)$$

We look for solutions that are expressible as products of a function of  $x$  alone,  $X(x)$ , a function of  $y$  alone,  $Y(y)$ , and a function of  $z$  alone,  $Z(z)$ .

$$\Phi = X(x)Y(y)Z(z) \quad (2)$$

Introducing (2) into (1) and dividing by  $\Phi$ , we obtain

$$\frac{1}{X} \frac{d^2 X}{dx^2} + \frac{1}{Y} \frac{d^2 Y}{dy^2} + \frac{1}{Z} \frac{d^2 Z}{dz^2} = 0 \quad (3)$$

A function of  $x$  alone, added to one of  $y$  alone and one of  $z$  alone, gives zero. Because  $x$ ,  $y$ , and  $z$  are independent variables, the zero sum is possible only if each of these three "functions" is in fact equal to a constant. The sum of these constants must then be zero.

$$\frac{1}{X} \frac{d^2 X}{dx^2} = -k_x^2; \quad \frac{1}{Y} \frac{d^2 Y}{dy^2} = k_y^2; \quad \frac{1}{Z} \frac{d^2 Z}{dz^2} = -k_z^2 \quad (4)$$

$$-k_x^2 + k_y^2 - k_z^2 = 0 \quad (5)$$

Note that if two of these three separation constants are positive, it is then necessary that the third be negative. We anticipated this by writing (4) accordingly. The solutions of (4) are

$$\begin{aligned} X &\sim \cos k_x x \quad \text{or} \quad \sin k_x x \\ Y &\sim \cosh k_y y \quad \text{or} \quad \sinh k_y y \\ Z &\sim \cos k_z z \quad \text{or} \quad \sin k_z z \end{aligned} \quad (6)$$

where

$$k_y^2 = k_x^2 + k_z^2.$$

Of course, the roles of the coordinates can be interchanged, so either the  $x$  or  $z$  directions could be taken as having the exponential dependence. From these solutions it is evident that the potential cannot be periodic or be exponential in its dependencies on all three coordinates and still be a solution to Laplace's equation. In writing (6) we have anticipated satisfying potential constraints on planes of constant  $y$  by taking  $X$  and  $Z$  as periodic.

**Modal Expansion in Cartesian Coordinates.** It is possible to choose the constants and the solutions from (6) so that zero potential boundary conditions are met on five of the six boundaries. With coordinates as shown in Fig. 5.10.1a, the sine functions are used for  $X$  and  $Z$  to insure a zero potential in the planes  $x = 0$  and  $z = 0$ . To make the potential zero in planes  $x = a$  and  $z = w$ , it is necessary that

$$\sin k_x a = 0; \quad \sin k_z w = 0 \quad (7)$$

Solution of these eigenvalue equations gives  $k_x = m\pi/a$ ,  $k_z = n\pi/w$ , and hence

$$XZ \sim \sin \frac{m\pi}{a} x \sin \frac{n\pi}{w} z \quad (8)$$

where  $m$  and  $n$  are integers.

To make the potential zero on the fifth boundary, say where  $y = 0$ , the hyperbolic sine function is used to represent the  $y$  dependence. Thus, a set of solutions, each meeting a zero potential condition on five boundaries, is

$$\Phi \sim \sin \frac{m\pi}{a} x \sin \frac{n\pi}{w} z \sinh k_{mn} y \quad (9)$$

where in view of (5)

$$k_{mn} \equiv \sqrt{(m\pi/a)^2 + (n\pi/w)^2}$$

These can be used to satisfy an arbitrary potential constraint on the "last" boundary, where  $y = b$ . The following example, which extends Sec. 5.5, illustrates this concept.

**Example 5.10.1.** Capacitive Attenuator in Three Dimensions

In the attenuator of Example 5.5.1, the two-dimensional field distribution is a good approximation because one cross-sectional dimension is small compared to the other. In Fig. 5.5.5,  $a \ll w$ . If the cross-sectional dimensions  $a$  and  $w$  are comparable, as shown in Fig. 5.10.2, the field can be represented by the modal superposition given by (9).

$$\Phi = \sum_{m=1}^{\infty} \sum_{n=1}^{\infty} A_{mn} \sin \frac{m\pi}{a} x \sin \frac{n\pi}{w} z \sinh k_{mn} y \quad (10)$$

In the five planes  $x = 0$ ,  $x = a$ ,  $y = 0$ ,  $z = 0$ , and  $z = w$  the potential is zero. In the plane  $y = b$ , it is constrained to be  $v$  by an electrode connected to a voltage source.



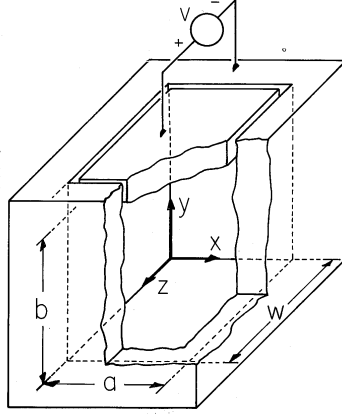


**Fig. 5.10.2** Region bounded by zero potentials at  $x = 0$ ,  $x = a$ ,  $z = 0$ ,  $z = w$ , and  $y = 0$ . Electrode constrains plane  $y = b$  to have potential  $v$ .

Evaluation of (10) at the electrode surface must give  $v$ .

$$v = \sum_{m=1}^{\infty} \sum_{n=1}^{\infty} A_{mn} \sinh k_{mn} b \sin \frac{m\pi}{a} x \sin \frac{n\pi}{w} z \quad (11)$$

The coefficients  $A_{mn}$  are determined by exploiting the orthogonality of the eigenfunctions. That is,

$$\int_0^a X_m X_i dx = \begin{cases} 0, & m \neq i \\ \frac{a}{2}, & m = i \end{cases}; \quad \int_0^w Z_n Z_j dz = \begin{cases} 0, & n \neq j \\ \frac{w}{2}, & n = j \end{cases} \quad (12)$$

where

$$X_m \equiv \sin \frac{m\pi}{a} x; \quad Z_n \equiv \sin \frac{n\pi}{w} z.$$

The steps that now lead to an expression for any given coefficient  $A_{mn}$  are a natural extension of those used in Sec. 5.5. Both sides of (11) are multiplied by the eigenfunction  $X_i Z_j$  and then both sides are integrated over the surface at  $y = b$ .

$$\int_0^a \int_0^w v X_i Z_j dx dz = \sum_{m=1}^{\infty} \sum_{n=1}^{\infty} A_{mn} \sinh(k_{mn} b) \int_0^a \int_0^w X_m X_i Z_n Z_j dx dz \quad (13)$$

Because of the product form of each term, the integrations can be carried out on  $x$  and  $z$  separately. In view of the orthogonality conditions, (12), the only non-zero term on the right comes in the summation with  $m = i$  and  $n = j$ . This makes it possible to solve the equation for the coefficient  $A_{ij}$ . Then, by replacing  $i \rightarrow m$  and  $j \rightarrow n$ , we obtain

$$A_{mn} = \frac{\int_0^a \int_0^w v \sin \frac{m\pi}{a} x \sin \frac{n\pi}{w} z dx dz}{\frac{aw}{4} \sinh(k_{mn} b)} \quad (14)$$

The integral can be carried out for any given distribution of potential. In this particular situation, the potential of the surface at  $y = b$  is uniform. Thus, integration gives

$$A_{mn} = \begin{cases} \frac{16v}{mn\pi^2} \frac{1}{\sinh(k_{mn}b)} & \text{for } m \text{ and } n \text{ both odd} \\ 0 & \text{for either } m \text{ or } n \text{ even} \end{cases} \quad (15)$$

The desired potential, satisfying the boundary conditions on all six surfaces, is given by (10) and (15). Note that the first term in the solution we have found is not the same as the first term in the two-dimensional field representation, (5.5.9). No matter what the ratio of  $a$  to  $w$ , the first term in the three-dimensional solution has a sinusoidal dependence on  $z$ , while the two-dimensional one has no dependence on  $z$ .

For the capacitive attenuator of Fig. 5.5.5, what output signal is predicted by this three dimensional representation? From (10) and (15), the charge on the output electrode is

$$q = \int_0^a \int_0^w \left[ -\epsilon_o \frac{\partial \Phi}{\partial y} \right]_{y=0} dx dz \equiv -C_M v \quad (16)$$

where

$$C_M = \frac{64}{\pi^4} \epsilon_o a w \sum_{\substack{m=1 \\ \text{odd}}}^{\infty} \sum_{\substack{n=1 \\ \text{odd}}}^{\infty} \frac{k_{mn}}{m^2 n^2 \sinh(k_{mn}b)}$$

With  $v = V \sin \omega t$ , we find that  $v_o = V_o \cos \omega t$  where

$$V_o = RC_n \omega V \quad (17)$$

Using (16), it follows that the amplitude of the output voltage is

$$\frac{V_o}{U'} = \sum_{\substack{m=1 \\ \text{odd}}}^{\infty} \sum_{\substack{n=1 \\ \text{odd}}}^{\infty} \frac{a k_{mn}}{2\pi m^2 n^2 \sinh \left[ (k_{mn}a) \frac{b}{a} \right]} \quad (18)$$

where the voltage is normalized to

$$U' = \frac{128\epsilon_o w R \omega V}{\pi^3}$$

and

$$k_{mn}a = \sqrt{(n\pi)^2 + (m\pi)^2 (a/w)^2}$$

This expression can be used to replace the plot of Fig. 5.5.5. Here we compare the two-dimensional and three-dimensional predictions of output voltage by considering (18) in the limit where  $b \gg a$ . In this limit, the hyperbolic sine is dominated by one of its exponentials, and the first term in the series gives

$$\ln\left(\frac{V_o}{U'}\right) \rightarrow \ln \sqrt{1 + (a/w)^2} - \pi \sqrt{1 + (a/w)^2} \frac{b}{a} \quad (19)$$

In the limit  $a/w \ll 1$ , the dependence on spacing between input and output electrodes expressed by the right hand side becomes identical to that for the two-dimensional model, (5.5.15). However,  $U' = (8/\pi^2)U$  regardless of  $a/w$ .

This three-dimensional Cartesian coordinate example illustrates how the orthogonality property of the product solution is exploited to provide a potential

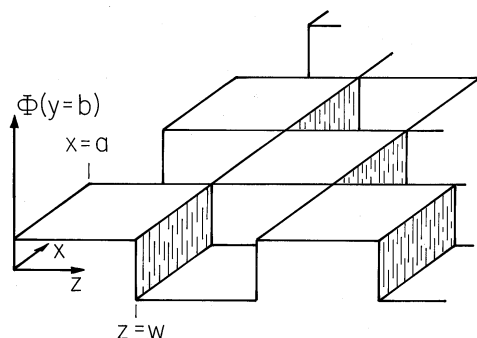


**Fig. 5.10.3** Two-dimensional square wave function used to represent electrode potential for system of Fig. 5.10.2 in plane  $y = b$ .

that is zero on five of the boundaries while assuming any desired distribution on the sixth boundary. On this sixth surface, the potential takes the form

$$\Phi = \sum_{\substack{m=1 \\ \text{odd}}}^{\infty} \sum_{\substack{n=1 \\ \text{odd}}}^{\infty} V_{mn} F_{mn} \quad (20)$$

where

$$F_{mn} \equiv X_m Z_n \equiv \sin \frac{m\pi}{a} x \sin \frac{n\pi}{w} z$$

The two-dimensional functions  $F_{mn}$  have been used to represent the “last” boundary condition. This two-dimensional Fourier series replaces the one-dimensional Fourier series of Sec. 5.5 (5.5.17). In the example, it represents the two-dimensional square wave function shown in Fig. 5.10.3. Note that this function goes to zero along  $x = 0$ ,  $x = a$  and  $z = 0$ ,  $z = w$ , as it should. It changes sign as it passes through any one of these “nodal” lines, but the range outside the original rectangle is of no physical interest, and hence the behavior outside that range does not affect the validity of the solution applied to the example. Because the function represented is odd in both  $x$  and  $y$ , it can be represented by sine functions only.

Our foray into three-dimensional modal expansions extends the notion of orthogonality of functions with respect to a one-dimensional interval to orthogonality of functions with respect to a two-dimensional section of a plane. We are able to determine the coefficients  $V_{mn}$  in (20) as it is made to fit the potential prescribed on the “sixth” surface because the terms in the series are orthogonal in the sense that

$$\int_0^a \int_0^w F_{mn} F_{ij} dx dz = \begin{cases} 0 & m \neq i \text{ or } n \neq j \\ \frac{aw}{4} & m = i \text{ and } n = j \end{cases} \quad (21)$$

In other coordinate systems, a similar orthogonality relation will hold for the product solutions evaluated on one of the surfaces defined by a constant natural coordinate. In general, a weighting function multiplies the eigenfunctions in the integrand of the surface integral that is analogous to (21).

Except for some special cases, this is as far as we will go in considering three-dimensional product solutions to Laplace’s equation. In the remainder of this section, references to the literature are given for solutions in cylindrical, spherical, and other coordinate systems.

**Modal Expansion in Other Coordinates.** A general volume having natural boundaries in cylindrical coordinates is shown in Fig. 5.10.1b. Product solutions to Laplace's equation take the form

$$\Phi = R(r)F(\phi)Z(z) \quad (22)$$

The polar coordinates of Sec. 5.7 are a special case where  $Z(z)$  is a constant.

The ordinary differential equations, analogous to (4) and (5), that determine  $F(\phi)$  and  $Z(z)$ , have constant coefficients, and hence the solutions are sines and cosines of  $m\phi$  and  $kz$ , respectively. The radial dependence is predicted by an ordinary differential equation that, like (5.7.5), has space-varying coefficients. Unfortunately, with the  $z$  dependence, solutions are not simply polynomials. Rather, they are Bessel's functions of order  $m$  and argument  $kr$ . As applied to product solutions to Laplace's equation, these functions are described in standard fields texts<sup>[1-4]</sup>. Bessel's and associated functions are developed in mathematics texts and treatises<sup>[5-8]</sup>.

As has been illustrated in two- and now three-dimensions, the solution to an arbitrary potential distribution on the boundaries can be written as the superposition of solutions each having the desired potential on one boundary and zero potential on the others. Summarized in Table 5.10.1 are the forms taken by the product solution, (22), in representing the potential for an arbitrary distribution on the specified surface. For example, if the potential is imposed on a surface of constant  $r$ , the radial dependence is given by Bessel's functions of real order and imaginary argument. What is needed to represent  $\Phi$  in the constant  $r$  surface are functions that are periodic in  $\phi$  and  $z$ , so we expect that these Bessel's functions have an exponential-like dependence on  $r$ .

In spherical coordinates, product solutions take the form

$$\Phi = R(r)\Theta(\theta)F(\phi) \quad (23)$$

From the cylindrical coordinate solutions, it might be guessed that new functions are required to describe  $R(r)$ . In fact, these turn out to be simple polynomials. The  $\phi$  dependence is predicted by a constant coefficient equation, and hence represented by familiar trigonometric functions. But the  $\theta$  dependence is described by Legendre functions. By contrast with the Bessel's functions, which are described by infinite polynomial series, the Legendre functions are finite polynomials in  $\cos(\theta)$ . In connection with Laplace's equation, the solutions are summarized in fields texts<sup>[1-4]</sup>. As solutions to ordinary differential equations, the Legendre polynomials are presented in mathematics texts<sup>[5,7]</sup>.

The names of other coordinate systems suggest the surfaces generated by setting one of the variables equal to a constant: Elliptic-cylinder coordinates and prolate spheroidal coordinates are examples in which Laplace's equation is separable<sup>[2]</sup>. The first step in exploiting these new systems is to write the Laplacian and other differential operators in terms of those coordinates. This is also described in the given references.

## 5.11 SUMMARY

There are two themes in this chapter. First is the division of a solution to a partial differential equation into a particular part, designed to balance the "drive" in the

TABLE 5.10.1 FORM OF SOLUTIONS TO LAPLACE'S EQUATION IN CYLINDRICAL COORDINATES WHEN POTENTIAL IS CONSTRAINED ON GIVEN SURFACE AND OTHERS ARE AT ZERO POTENTIAL			
Surface of Constant	$R(r)$	$F(\phi)$	$Z(z)$
$r$	Bessel's functions of real order and imaginary argument (modified Bessel's functions)	trigonometric functions of real argument	trigonometric functions of real argument
$\phi$	Bessel's functions of imaginary order and imaginary argument	trigonometric functions of imaginary argument	trigonometric functions of real argument
$z$	Bessel's functions of real order and real argument	trigonometric functions of real argument	trigonometric functions of imaginary argument

differential equation, and a homogeneous part, used to make the total solution satisfy the boundary conditions. This chapter solves Poisson's equation; the "drive" is due to the volumetric charge density and the boundary conditions are stated in terms of prescribed potentials. In the following chapters, the approach used here will be applied to boundary value problems representing many different physical situations. Differential equations and boundary conditions will be different, but because they will be linear, the same approach can be used.

Second is the theme of product solutions to Laplace's equation which by virtue of their orthogonality can be superimposed to satisfy arbitrary boundary conditions. The thrust of this statement can be appreciated by the end of Sec. 5.5. In the configuration considered in that section, the potential is zero on all but one of the natural Cartesian boundaries of an enclosed region. It is shown that the product solutions can be superimposed to satisfy an arbitrary potential condition on the "last" boundary. By making the "last" boundary any one of the boundaries and, if need be, superimposing as many series solutions as there are boundaries, it is then possible to meet arbitrary conditions on all of the boundaries. The section on polar coordinates gives the opportunity to extend these ideas to systems where the coordinates are not interchangeable, while the section on three-dimensional Cartesian solutions indicates a typical generalization to three dimensions.

In the chapters that follow, there will be a frequent need for solving Laplace's equation. To this end, three classes of solutions will often be exploited: the Cartesian solutions of Table 5.4.1, the polar coordinate ones of Table 5.7.1, and the three

spherical coordinate solutions of Sec. 5.9. In Chap. 10, where magnetic diffusion phenomena are introduced and in Chap. 13, where electromagnetic waves are described, the application of these ideas to the diffusion and the Helmholtz equations is illustrated.

## REFERENCES

- [1] M. Zahn, **Electromagnetic Field Theory: A Problem Solving Approach**, John Wiley and Sons, N.Y. (1979).
- [2] P. Moon and D. E. Spencer, **Field Theory for Engineers**, Van Nostrand, Princeton, N.J. (1961).
- [3] S. Ramo, J. R. Whinnery, and T. Van Duzer, **Fields and Waves in Communication Electronics**, John Wiley and Sons, N.Y. (1967).
- [4] J. R. Melcher, **Continuum Electromechanics**, M.I.T. Press, Cambridge, Mass. (1981).
- [5] F. B. Hildebrand, **Advanced Calculus for Applications**, Prentice-Hall, Inc, Englewood Cliffs, N.J. (1962).
- [6] G. N. Watson, **A Treatise on the Theory of Bessel Functions**, Cambridge University Press, London E.C.4. (1944).
- [7] P. M. Morse and H. Feshbach, **Methods of Theoretical Physics**, McGraw-Hill Book Co., N.Y. (1953).
- [8] N. W. McLachlan, **Bessel Functions for Engineers**, Oxford University Press, London E.C.4 (1941).

## P R O B L E M S

## 5.1 Particular and Homogeneous Solutions to Poisson's and Laplace's Equations

5.1.1 In Problem 4.7.1, the potential of a point charge over a perfectly conducting plane (where  $z > 0$ ) was found to be Eq. (a) of that problem. Identify particular and homogeneous parts of this solution.

5.1.2 A solution for the potential in the region  $-a < y < a$ , where there is a charge density  $\rho$ , satisfies the boundary conditions  $\Phi = 0$  in the planes  $y = +a$  and  $y = -a$ .

$$\Phi = \frac{\rho_o}{\epsilon_o \beta^2} \left( 1 - \frac{\cosh \beta y}{\cosh \beta a} \right) \cos \beta x \quad (a)$$

- What is  $\rho$  in this region?
- Identify  $\Phi_p$  and  $\Phi_h$ . What boundary conditions are satisfied by  $\Phi_h$  at  $y = +a$  and  $y = -a$ ?
- Illustrate another combination of  $\Phi_p$  and  $\Phi_h$  that could just as well be used and give the boundary conditions that apply for  $\Phi_h$  in that case.

5.1.3\* The charge density between the planes  $x = 0$  and  $x = d$  depends only on  $x$ .

$$\rho = \frac{4\rho_o(x-d)^2}{d^2} \quad (a)$$

Boundary conditions are that  $\Phi(x = 0) = 0$  and  $\Phi(x = d) = V$ , so  $\Phi = \Phi(x)$  is independent of  $y$  and  $z$ .

- Show that Poisson's equation therefore reduces to

$$\frac{\partial^2 \Phi}{\partial x^2} = -\frac{4\rho_o}{d^2 \epsilon_o} (x-d)^2 \quad (b)$$

- Integrate this expression twice and use the boundary conditions to show that the potential distribution is

$$\Phi = -\frac{\rho_o}{3d^2 \epsilon_o} (x-d)^4 + \left( \frac{V}{d} - \frac{\rho_o d}{3\epsilon_o} \right) x + \frac{\rho_o d^2}{3\epsilon_o} \quad (c)$$

- Argue that the first term in (c) can be  $\Phi_p$ , with the remaining terms then  $\Phi_h$ .
- Show that in that case, the boundary conditions satisfied by  $\Phi_h$  are

$$\Phi_h(0) = \frac{\rho_o d^2}{3\epsilon_o}; \quad \Phi_h(d) = V \quad (d)$$

5.1.4 With the charge density given as

$$\rho = \rho_o \sin \frac{\pi x}{d} \tag{a}$$

carry out the steps in Prob. 5.1.3.

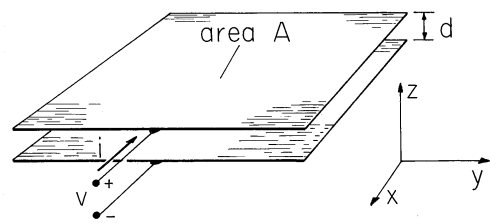


Fig. P5.1.5

5.1.5\* A frequently used model for a capacitor is shown in Fig. P5.1.5, where two plane parallel electrodes have a spacing that is small compared to either of their planar dimensions. The potential difference between the electrodes is  $v$ , and so over most of the region between the electrodes, the electric field is uniform.

- (a) Show that in the region well removed from the edges of the electrodes, the field  $\mathbf{E} = -(v/d)\mathbf{i}_z$  satisfies Laplace's equation and the boundary conditions on the electrode surfaces.
- (b) Show that the surface charge density on the lower surface of the upper electrode is  $\sigma_s = \epsilon_o v/d$ .
- (c) For a single pair of electrodes, the capacitance  $C$  is defined such that  $q = Cv$  (13). Show that for the plane parallel capacitor of Fig. P5.1.5,  $C = A\epsilon_o/d$ , where  $A$  is the area of one of the electrodes.
- (d) Use the integral form of charge conservation, (1.5.2), to show that  $i = dq/dt = Cdv/dt$ .

5.1.6\* In the three-electrode system of Fig. P5.1.6, the bottom electrode is taken as having the reference potential. The upper and middle electrodes then have potentials  $v_1$  and  $v_2$ , respectively. The spacings between electrodes,  $2d$  and  $d$ , are small enough relative to the planar dimensions of the electrodes so that the fields between can be approximated as being uniform.

- (a) Show that the fields denoted in the figure are then approximately  $E_1 = v_1/2d$ ,  $E_2 = v_2/d$  and  $E_m = (v_1 - v_2)/d$ .
- (b) Show that the net charges  $q_1$  and  $q_2$  on the top and middle electrodes, respectively, are related to the voltages by the capacitance matrix [in the form of (12)]

$$\begin{bmatrix} q_1 \\ q_2 \end{bmatrix} = \begin{bmatrix} \epsilon_o w(L+l)/2d & -\epsilon_o wl/d \\ -\epsilon_o wl/d & 2\epsilon_o wl/d \end{bmatrix} \begin{bmatrix} v_1 \\ v_2 \end{bmatrix} \tag{a}$$



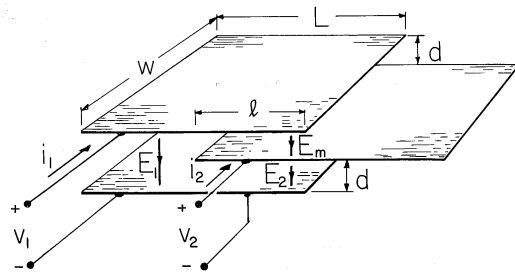


Fig. P5.1.6

### 5.3 Continuity Conditions

5.3.1\* The electric potentials  $\Phi^a$  and  $\Phi^b$  above and below the plane  $y = 0$  are

$$\begin{aligned}\Phi^a &= V \cos \beta x \exp(-\beta y); & y > 0 \\ \Phi^b &= V \cos \beta x \exp(\beta y); & y < 0\end{aligned}\quad (a)$$

- Show that (4) holds. (The potential is continuous at  $y = 0$ .)
- Evaluate  $\mathbf{E}$  tangential to the surface  $y = 0$  and show that it too is continuous. [Equation (1) is then automatically satisfied at  $y = 0$ .]
- Use (5) to show that in the plane  $y = 0$ , the surface charge density,  $\sigma_s = 2\epsilon_0\beta V \cos \beta x$ , accounts for the discontinuity in the derivative of  $\Phi$  normal to the plane  $y = 0$ .

5.3.2 By way of appreciating how the continuity of  $\Phi$  guarantees the continuity of tangential  $\mathbf{E}$  [(4) implies that (1) is satisfied], suppose that the potential is given in the plane  $y = 0$ :  $\Phi = \Phi(x, 0, z)$ .

- Which components of  $\mathbf{E}$  can be determined from this information alone?
- For example, if  $\Phi(x, 0, z) = V \sin(\beta x) \sin(\beta z)$ , what are those components of  $\mathbf{E}$ ?

### 5.4 Solutions to Laplace's Equation in Cartesian Coordinates

5.4.1\* A region that extends to  $\pm\infty$  in the  $z$  direction has the square cross-section of dimensions as shown in Fig. P5.4.1. The walls at  $x = 0$  and  $y = 0$  are at zero potential, while those at  $x = a$  and  $y = a$  have the linear distributions shown. The interior region is free of charge density.

- Show that the potential inside is

$$\Phi = \frac{V_o xy}{a^2}\quad (a)$$

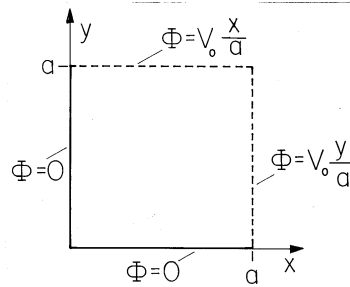


Fig. P5.4.1

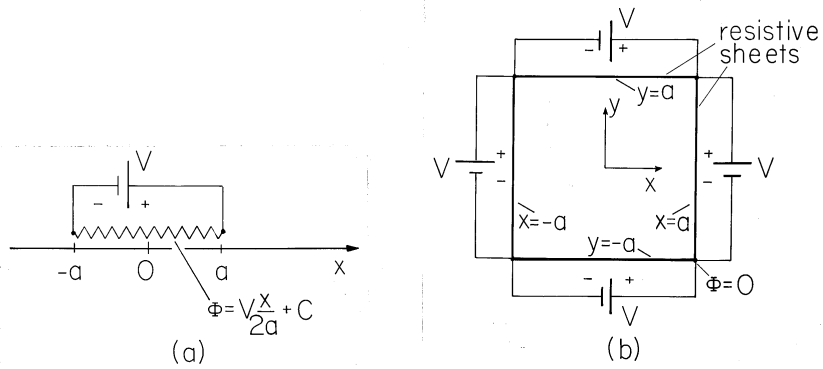


Fig. P5.4.2

(b) Show that plots of  $\Phi$  and  $\mathbf{E}$  are as shown in the first quadrant of Fig. 4.1.3.

**5.4.2** One way to constrain a boundary so that it has a potential distribution that is a linear function of position is shown in Fig. P5.4.2a. A uniformly resistive sheet having a length  $2a$  is driven by a voltage source  $V$ . For the coordinate  $x$  shown, the resulting potential distribution is the linear function of  $x$  shown. The constant  $C$  is determined by the definition of where the potential is zero. In the case shown in Fig. 5.4.2a, if  $\Phi$  is zero at

$x = 0$ , then  $C = 0$ .

- (a) Suppose a cylindrical region having a square cross-section of length  $2a$  on a side, as shown in Fig. 5.4.2b, is constrained in potential by resistive sheets and voltage sources, as shown. Note that the potential is defined to be zero at the lower right-hand corner, where  $(x, y) = (a, -a)$ . Inside the cylinder, what must the potential be in the planes  $x = \pm a$  and  $y = \pm a$ ?
- (b) Find the linear combination of the potentials from the first column of Table 5.4.1 that satisfies the conditions on the potentials required by the resistive sheets. That is, if  $\Phi$  takes the form

$$\Phi = Ax + By + C + Dxy \quad (a)$$

so that it satisfies Laplace's equation inside the cylinder, what are the coefficients  $A$ ,  $B$ ,  $C$ , and  $D$ ?

- (c) Determine  $\mathbf{E}$  for this potential.
- (d) Sketch  $\Phi$  and  $\mathbf{E}$ .
- (e) Now the potential on the walls of the square cylinder is constrained as shown in Fig. 5.4.2c. This time the potential is zero at the location  $(x, y) = (0, 0)$ . Adjust the coefficients in (a) so that the potential satisfies these conditions. Determine  $\mathbf{E}$  and sketch the equipotentials and field lines.

**5.4.3\*** Shown in cross-section in Fig. P5.4.3 is a cylindrical system that extends to infinity in the  $\pm z$  directions. There is no charge density inside the cylinder, and the potentials on the boundaries are

$$\Phi = V_o \cos \frac{\pi x}{a} \quad \text{at} \quad y = \pm b \quad (a)$$

$$\Phi = 0 \quad \text{at} \quad x = \pm \frac{a}{2} \quad (b)$$

- (a) Show that the potential inside the cylinder is

$$\Phi = V_o \cos \frac{\pi x}{a} \cosh \frac{\pi y}{a} / \cosh \frac{\pi b}{a} \quad (c)$$

- (b) Show that a plot of  $\Phi$  and  $\mathbf{E}$  is as given by the part of Fig. 5.4.1 where  $-\pi/2 < kx < \pi/2$ .

**5.4.4** The square cross-section of a cylindrical region that extends to infinity in the  $\pm z$  directions is shown in Fig. P5.4.4. The potentials on the boundaries are as shown.

- (a) Inside the cylindrical space, there is no charge density. Find  $\Phi$ .
- (b) What is  $\mathbf{E}$  in this region?

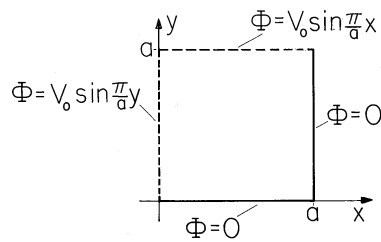


Fig. P5.4.4

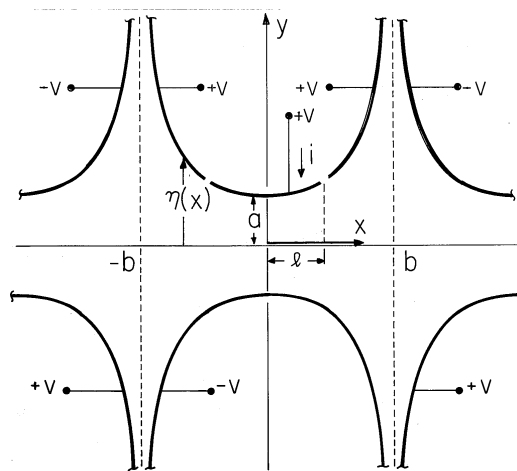


Fig. P5.4.5

(c) Sketch  $\Phi$  and  $\mathbf{E}$ .

5.4.5\* The cross-section of an electrode structure which is symmetric about the  $x = 0$  plane is shown in Fig. P5.4.5. Above this plane are electrodes that alternately either have the potential  $v(t)$  or the potential  $-v(t)$ . The system has depth  $d$  (into the paper) which is very long compared to such dimensions as  $a$  or  $l$ . So that the current  $i(t)$  can be measured, one of the upper electrodes has a segment which is insulated from the rest of the electrode, but driven by the same potential. The geometry of the upper electrodes is specified by giving their altitudes above the  $x = 0$  plane. For example, the upper electrode between  $y = -b$  and  $y = b$  has the shape

$$\eta = \frac{1}{k} \sinh^{-1} \left( \frac{\sinh ka}{\cos kx} \right); \quad k = \frac{\pi}{2b} \tag{a}$$

where  $\eta$  is as shown in Fig. P5.4.5.

(a) Show that the potential in the region between the electrodes is

$$\Phi = v(t) \cos kx \sinh ky / \sinh ka \tag{b}$$

(b) Show that  $\mathbf{E}$  in this region is

$$\mathbf{E} = \frac{v(t)}{\sinh\left(\frac{\pi a}{2b}\right)} \left(\frac{\pi}{2b}\right) \left[ \sin\left(\frac{\pi x}{2b}\right) \sinh\left(\frac{\pi y}{2b}\right) \mathbf{i}_x - \cos\left(\frac{\pi x}{2b}\right) \cosh\left(\frac{\pi y}{2b}\right) \mathbf{i}_y \right] \quad (c)$$

(c) Show that plots of  $\Phi$  and  $\mathbf{E}$  are as shown in Fig. 5.4.2.

(d) Show that the net charge on the upper electrode segment between  $y = -l$  and  $y = l$  is

$$q = \frac{2\epsilon_0 d}{\sinh ka} \sin kl \left[ 1 + \left(\frac{\sinh ka}{\cos kl}\right)^2 \right]^{1/2} v(t) = Cv \quad (d)$$

(Because the surface  $S$  in Gauss' integral law is arbitrary, it can be chosen so that it both encloses this electrode and is convenient for integration.)

(e) Given that  $v(t) = V_o \sin \omega t$ , where  $V_o$  and  $\omega$  are constants, show that the current to the electrode segment  $i(t)$ , as defined in Fig. P5.4.5, is

$$i = \frac{dq}{dt} = C \frac{dv}{dt} = C\omega V_o \cos \omega t \quad (e)$$

**5.4.6** In Prob. 5.4.5, the polarities of all of the voltage sources driving the lower electrodes are reversed.

- Find  $\Phi$  in the region between the electrodes.
- Determine  $\mathbf{E}$ .
- Sketch  $\Phi$  and  $\mathbf{E}$ .
- Find the charge  $q$  on the electrode segment in the upper middle electrode.
- Given that  $v(t) = V_o \cos \omega t$ , what is  $i(t)$ ?

## 5.5 Modal Expansion to Satisfy Boundary Conditions

**5.5.1\*** The system shown in Fig. P5.5.1a is composed of a pair of perfectly conducting parallel plates in the planes  $x = 0$  and  $x = a$  that are shorted in the plane  $y = b$ . Along the left edge, the potential is imposed and so has a given distribution  $\Phi_d(x)$ . The plates and short have zero potential.

(a) Show that, in terms of  $\Phi_d(x)$ , the potential distribution for  $0 < y < b$ ,  $0 < x < a$  is

$$\Phi = \sum_{n=1}^{\infty} A_n \sin\left(\frac{n\pi x}{a}\right) \sinh\left[\frac{n\pi}{a}(y-b)\right] \quad (a)$$

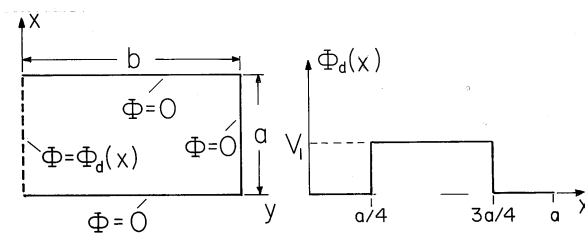


Fig. P5.5.1

where

$$A_n = \frac{2}{a \sinh\left(-\frac{n\pi b}{a}\right)} \int_0^a \Phi_d(x) \sin\left(\frac{n\pi x}{a}\right) dx \quad (b)$$

(At this stage, the coefficients in a modal expansion for the field are left expressed as integrals over the yet to be specified potential distribution.)

- (b) In particular, if the imposed potential is as shown in Fig. P5.5.1b, show that  $A_n$  is

$$A_n = -\frac{4V_1}{n\pi} \frac{\cos\left(\frac{n\pi}{4}\right)}{\sinh\left(\frac{n\pi b}{a}\right)} \quad (c)$$

**5.5.2\*** The walls of a rectangular cylinder are constrained in potential as shown in Fig. P5.5.2. The walls at  $x = a$  and  $y = b$  have zero potential, while those at  $y = 0$  and  $x = 0$  have the potential distributions  $V_1(x)$  and  $V_2(y)$ , respectively.

In particular, suppose that these distributions of potential are uniform, so that  $V_1(x) = V_a$  and  $V_2(y) = V_b$ , with  $V_a$  and  $V_b$  defined to be independent of  $x$  and  $y$ .

- (a) The region inside the cylinder is free space. Show that the potential distribution there is

$$\Phi = \sum_{\substack{n=1 \\ \text{odd}}}^{\infty} \left[ -\frac{4V_b}{n\pi} \frac{\sinh\frac{n\pi}{b}(x-a)}{\sinh\frac{n\pi a}{b}} \sin\frac{n\pi y}{b} - \frac{4V_a}{n\pi} \frac{\sinh\frac{n\pi}{a}(y-b)}{\sinh\frac{n\pi b}{a}} \sin\frac{n\pi x}{a} \right] \quad (a)$$

- (b) Show that the distribution of surface charge density along the wall at  $x = a$  is

$$\sigma_s = \sum_{\substack{n=1 \\ \text{odd}}}^{\infty} \left[ -\frac{4\epsilon_o V_b}{b} \frac{\sin\frac{n\pi}{b}y}{\sinh\frac{n\pi a}{b}} + \frac{4\epsilon_o V_a}{a} \frac{\sinh\frac{n\pi}{a}(y-b)}{\sinh\frac{n\pi b}{a}} \right] \quad (b)$$

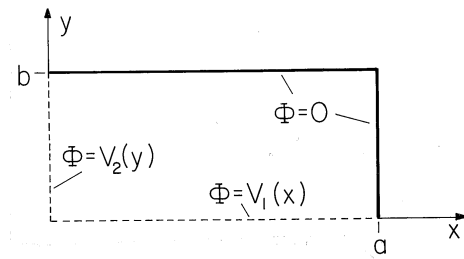


Fig. P5.5.2

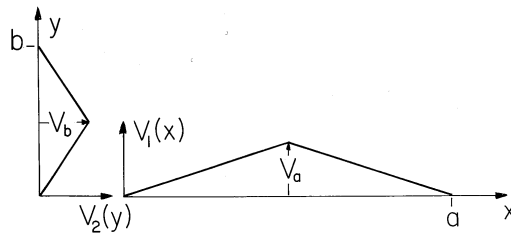


Fig. P5.5.3

5.5.3 In the configuration described in Prob. 5.5.2, the distributions of potentials on the walls at  $x = 0$  and  $y = 0$  are as shown in Fig. P5.5.3, where the peak voltages  $V_a$  and  $V_b$  are given functions of time.

- (a) Determine the potential in the free space region inside the cylinder.
- (b) Find the surface charge distribution on the wall at  $y = b$ .

5.5.4\* The cross-section of a system that extends to “infinity” out of the paper is shown in Fig. P5.5.4. An electrode in the plane  $y = d$  has the potential  $V$ . A second electrode has the shape of an “L.” One of its sides is in the plane  $y = 0$ , while the other is in the plane  $x = 0$ , extending from  $y = 0$  almost to  $y = d$ . This electrode is at zero potential.

- (a) The electrodes extend to infinity in the  $-x$  direction. Show that, far to the left, the potential between the electrodes tends to

$$\Phi = \frac{Vy}{d} \tag{a}$$

- (b) Using this result as a part of the solution,  $\Phi_a$ , the potential between the plates is written as  $\Phi = \Phi_a + \Phi_b$ . Show that the boundary conditions that must be satisfied by  $\Phi_b$  are

$$\Phi_b = 0 \quad \text{at } y = 0 \quad \text{and } y = d \tag{b}$$

$$\Phi_b \rightarrow 0 \quad \text{as } x \rightarrow -\infty \tag{c}$$

$$\Phi_b = -\frac{Vy}{d} \quad \text{at } x = 0 \tag{d}$$

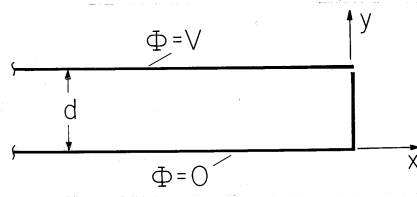


Fig. P5.5.4

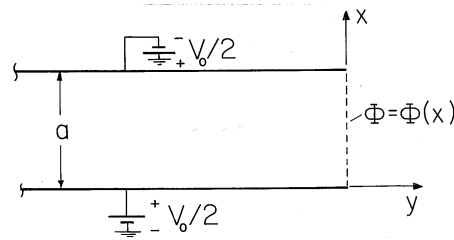


Fig. P5.5.5

(c) Show that the potential between the electrodes is

$$\Phi = \frac{Vy}{d} + \sum_{n=1}^{\infty} \frac{2V}{n\pi} (-1)^n \sin \frac{n\pi y}{d} \exp\left(-\frac{n\pi x}{d}\right) \quad (e)$$

(d) Show that a plot of  $\Phi$  and  $\mathbf{E}$  appears as shown in Fig. 6.6.9c, turned upside down.

**5.5.5** In the two-dimensional system shown in cross-section in Fig. P5.5.5, plane parallel plates extend to infinity in the  $-y$  direction. The potentials of the upper and lower plates are, respectively,  $-V_0/2$  and  $V_0/2$ . The potential over the plane  $y = 0$  terminating the plates at the right is specified to be  $\Phi_d(x)$ .

- (a) What is the potential distribution between the plates far to the left?
- (b) If  $\Phi$  is taken as the potential  $\Phi_a$  that assumes the correct distribution as  $y \rightarrow -\infty$ , plus a potential  $\Phi_b$ , what boundary conditions must be satisfied by  $\Phi_b$ ?
- (c) What is the potential distribution between the plates?

**5.5.6** As an alternative (and in this case much more complicated) way of expressing the potential in Prob. 5.4.1, use a modal approach to express the potential in the interior region of Fig. P5.4.1.

**5.5.7\*** Take an approach to finding the potential in the configuration of Fig. 5.5.2 that is an alternative to that used in the text. Let  $\Phi = (Vy/b) + \Phi_1$ .

- (a) Show that the boundary conditions that must be satisfied by  $\Phi_1$  are that  $\Phi_1 = -Vy/b$  at  $x = 0$  and at  $x = a$ , and  $\Phi_1 = 0$  at  $y = 0$  and  $y = b$ .



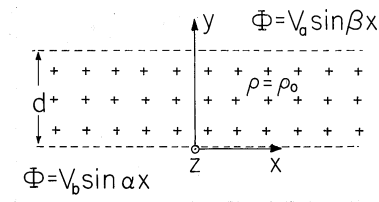


Fig. P5.6.1

(b) Show that the potential is

$$\Phi = \frac{Vy}{b} + \sum_{n=1}^{\infty} A_n \cosh \frac{n\pi}{b} \left(x - \frac{a}{2}\right) \sin \frac{n\pi y}{b} \tag{a}$$

where

$$A_n = \frac{2V(-1)^n}{\cosh \left(\frac{n\pi a}{2b}\right)} \tag{b}$$

(It is convenient to exploit the symmetry of the configuration about the plane  $x = a/2$ .)

### 5.6 Solutions to Poisson's Equation with Boundary Conditions

**5.6.1\*** The potential distribution is to be determined in a region bounded by the planes  $y = 0$  and  $y = d$  and extending to infinity in the  $x$  and  $z$  directions, as shown in Fig. P5.6.1. In this region, there is a uniform charge density  $\rho_0$ . On the upper boundary, the potential is  $\Phi(x, d, z) = V_a \sin(\beta x)$ . On the lower boundary,  $\Phi(x, 0, z) = V_b \sin(\alpha x)$ . Show that  $\Phi(x, y, z)$  throughout the region  $0 < y < d$  is

$$\begin{aligned} \Phi = & V_a \sin \beta x \frac{\sinh \beta y}{\sinh \beta d} - V_b \sin \alpha x \frac{\sinh \alpha(y-d)}{\sinh \alpha d} \\ & - \frac{\rho_0}{\epsilon_0} \left(\frac{y^2}{2} - \frac{yd}{2}\right) \end{aligned} \tag{a}$$

**5.6.2** For the configuration of Fig. P5.6.1, the charge is again uniform in the region between the boundaries, with density  $\rho_0$ , but the potential at  $y = d$  is  $\Phi = \Phi_0 \sin(kx)$ , while that at  $y = 0$  is zero ( $\Phi_0$  and  $k$  are given constants). Find  $\Phi$  in the region where  $0 < y < d$ , between the boundaries.

**5.6.3\*** In the region between the boundaries at  $y = \pm d/2$  in Fig. P5.6.3, the charge density is

$$\rho = \rho_0 \cos k(x - \delta); \quad -\frac{d}{2} < y < \frac{d}{2} \tag{a}$$

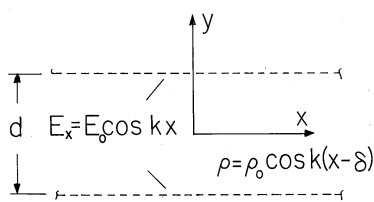


Fig. P5.6.3

where  $\rho_o$  and  $\delta$  are given constants. Electrodes at  $y = \pm d/2$  constrain the tangential electric field there to be

$$E_x = E_o \cos kx \quad (b)$$

The charge density might represent a traveling wave of space charge on a modulated particle beam, and the walls represent the traveling-wave structure which interacts with the beam. Thus, in a practical device, such as a traveling-wave amplifier designed to convert the kinetic energy of the moving charge to ac electrical energy available at the electrodes, the charge and potential distributions move to the right with the same velocity. This does not concern us, because we consider the interaction at one instant in time.

(a) Show that a particular solution is

$$\Phi_p = \frac{\rho_o}{\epsilon_o k^2} \cos k(x - \delta) \quad (c)$$

(b) Show that the total potential is the sum of this solution and that solution to Laplace's equation that makes the total solution satisfy the boundary conditions.

$$\Phi = \Phi_p - \frac{\cosh ky}{\cosh(kd/2)} \left[ \frac{E_o}{k} \sin kx + \frac{\rho_o}{\epsilon_o k^2} \cos k(x - \delta) \right] \quad (d)$$

(c) The force density (force per unit volume) acting on the charge is  $\rho \mathbf{E}$ . Show that the force  $f_x$  acting on a section of the charge of length in the  $x$  direction  $\lambda = 2\pi/k$  spanning the region  $-d/2 < y < d/2$  and unit length in the  $z$  direction is

$$f_x = \frac{2\pi\rho_o E_o}{k^2} \tanh\left(\frac{kd}{2}\right) \cos k\delta \quad (e)$$

**5.6.4** In the region  $0 < y < d$  shown in cross-section in Fig. P5.6.4, the charge density is

$$\rho = \rho_o \cos k(x - \delta); \quad 0 < y < d \quad (a)$$

where  $\rho_o$  and  $\delta$  are constants. Electrodes at  $y = d$  constrain the potential there to be  $\Phi(x, d) = V_o \cos(kx)$  ( $V_o$  and  $k$  given constants), while an electrode at  $y = 0$  makes  $\Phi(x, 0) = 0$ .

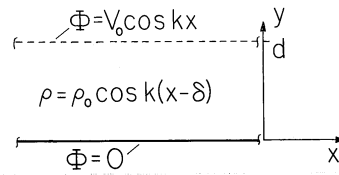


Fig. P5.6.4

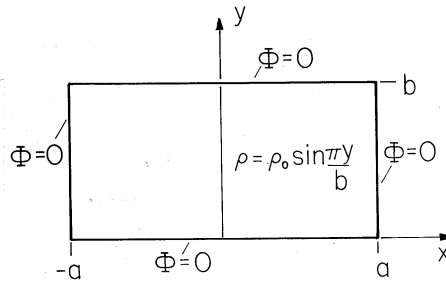


Fig. P5.6.5

- (a) Find a particular solution that satisfies Poisson's equation everywhere between the electrodes.
- (b) What boundary conditions must the homogeneous solution satisfy at  $y = d$  and  $y = 0$ ?
- (c) Find  $\Phi$  in the region  $0 < y < d$ .
- (d) The force density (force per unit volume) acting on the charge is  $\rho\mathbf{E}$ . Find the total force  $f_x$  acting on a section of the charge spanning the system from  $y = 0$  to  $y = d$ , of unit length in the  $z$  direction and of length  $\lambda = 2\pi/k$  in the  $x$  direction.

5.6.5\* A region that extends to infinity in the  $\pm z$  directions has a rectangular cross-section of dimensions  $2a$  and  $b$ , as shown in Fig. P5.6.5. The boundaries are at zero potential while the region inside has the distribution of charge density

$$\rho = \rho_0 \sin\left(\frac{\pi y}{b}\right) \tag{a}$$

where  $\rho_0$  is a given constant. Show that the potential in this region is

$$\Phi = \frac{\rho_0}{\epsilon_0} (b/\pi)^2 \sin\left(\frac{\pi y}{b}\right) \left[1 - \cosh \frac{\pi x}{b} / \cosh \frac{\pi a}{b}\right] \tag{b}$$

5.6.6 The cross-section of a two-dimensional configuration is shown in Fig. P5.6.6. The potential distribution is to be determined inside the boundaries, which are all at zero potential.

- (a) Given that a particular solution inside the boundaries is

$$\Phi_p = V \sin\left(\frac{\pi y}{b}\right) \sin \beta x \tag{a}$$

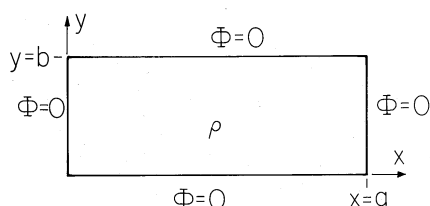


Fig. P5.6.6

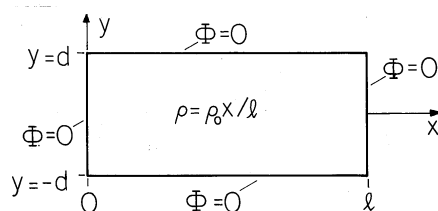


Fig. P5.6.7

where  $V$  and  $\beta$  are given constants, what is the charge density in that region?

(b) What is  $\Phi$ ?

**5.6.7** The cross-section of a metal box that is very long in the  $z$  direction is shown in Fig. P5.6.7. It is filled by the charge density  $\rho_0 x/l$ . Determine  $\Phi$  inside the box, given that  $\Phi = 0$  on the walls.

**5.6.8\*** In region (b), where  $y < 0$ , the charge density is  $\rho = \rho_0 \cos(\beta x)e^{\alpha y}$ , where  $\rho_0, \beta$ , and  $\alpha$  are positive constants. In region (a), where  $0 < y$ ,  $\rho = 0$ .

(a) Show that a particular solution in the region  $y < 0$  is

$$\Phi_p = \frac{\rho_0}{\epsilon_0(\beta^2 - \alpha^2)} \cos(\beta x) \exp(\alpha y) \quad (a)$$

(b) There is no surface charge density in the plane  $y = 0$ . Show that the potential is

$$\Phi = \frac{-\rho_0 \cos \beta x}{\epsilon_0(\beta^2 - \alpha^2)2} \begin{cases} \left(\frac{\alpha}{\beta} - 1\right) \exp(-\beta y); & 0 < y \\ -2 \exp(\alpha y) + \left(\frac{\alpha}{\beta} + 1\right) \exp(\beta y); & y < 0 \end{cases} \quad (b)$$

**5.6.9** A sheet of charge having the surface charge density  $\sigma_s = \sigma_0 \sin \beta(x - x_0)$  is in the plane  $y = 0$ , as shown in Fig. 5.6.3. At a distance  $a$  above and below the sheet, electrode structures are used to constrain the potential to be  $\Phi = V \cos \beta x$ . The system extends to infinity in the  $x$  and  $z$  directions. The regions above and below the sheet are designated (a) and (b), respectively.

(a) Find  $\Phi_a$  and  $\Phi_b$  in terms of the constants  $V, \beta, \sigma_0$ , and  $x_0$ .

- (b) Given that the force per unit area acting on the charge sheet is  $\sigma_s E_x(x, 0)$ , what is the force acting on a section of the sheet having length  $d$  in the  $z$  direction and one wavelength  $2\pi/\beta$  in the  $x$  direction?
- (c) Now, the potential on the wall is made a traveling wave having a given angular frequency  $\omega$ ,  $\Phi(x, \pm a, t) = V \cos(\beta x - \omega t)$ , and the charge moves to the right with a velocity  $U$ , so that  $\sigma_s = \sigma_o \sin \beta(x - Ut - x_o)$ , where  $U = \omega/\beta$ . Thus, the wall potentials and surface charge density move in synchronism. Building on the results from parts (a)–(b), what is the potential distribution and hence total force on the section of charged sheet?
- (d) What you have developed is a primitive model for an electron beam device used to convert the kinetic energy of the electrons (accelerated to the velocity  $v$  by a dc voltage) to high-frequency electrical power output. Because the system is free of dissipation, the electrical power output (through the electrode structure) is equal to the mechanical power input. Based on the force found in part (c), what is the electrical power output produced by one period  $2\pi/\beta$  of the charge sheet of width  $w$ ?
- (e) For what values of  $x_o$  would the device act as a generator of electrical power?

## 5.7 Solutions to Laplace's Equation in Polar Coordinates

- 5.7.1\* A circular cylindrical surface  $r = a$  has the potential  $\Phi = V \sin 5\phi$ . The regions  $r < a$  and  $a < r$  are free of charge density. Show that the potential is

$$\Phi = V \begin{cases} (r/a)^5 \sin 5\phi & r < a \\ (a/r)^5 \sin 5\phi & a < r \end{cases} \quad (a)$$

- 5.7.2 The  $x - z$  plane is one of zero potential. Thus, the  $y$  axis is perpendicular to a zero potential plane. With  $\phi$  measured relative to the  $x$  axis and  $z$  the third coordinate axis, the potential on the surface at  $r = R$  is constrained by segmented electrodes there to be  $\Phi = V \sin \phi$ .

- (a) If  $\rho = 0$  in the region  $r < R$ , what is  $\Phi$  in that region?
- (b) Over the range  $r < R$ , what is the surface charge density on the surface at  $y = 0$ ?

- 5.7.3\* An annular region  $b < r < a$  where  $\rho = 0$  is bounded from outside at  $r = a$  by a surface having the potential  $\Phi = V_a \cos 3\phi$  and from the inside at  $r = b$  by a surface having the potential  $\Phi = V_b \sin \phi$ . Show that  $\Phi$  in the annulus can be written as the sum of two terms, each a combination of solutions to Laplace's equation designed to have the correct value at one radius while

being zero at the other.

$$\Phi = V_a \cos 3\phi \frac{[(r/b)^3 - (b/r)^3]}{[(a/b)^3 - (b/a)^3]} + V_b \sin \phi \frac{[(r/a) - (a/r)]}{[(b/a) - (a/b)]} \quad (a)$$

**5.7.4** In the region  $b < r < a$ ,  $0 < \phi < \alpha$ ,  $\rho = 0$ . On the boundaries of this region at  $r = a$ , at  $\phi = 0$  and  $\phi = \alpha$ ,  $\Phi = 0$ . At  $r = b$ ,  $\Phi = V_b \sin(\pi\phi/\alpha)$ . Determine  $\Phi$  in this region.

**5.7.5\*** In the region  $b < r < a$ ,  $0 < \phi < \alpha$ ,  $\rho = 0$ . On the boundaries of this region at  $r = a$ ,  $r = b$  and at  $\phi = 0$ ,  $\Phi = 0$ . At  $\phi = \alpha$ , the potential is  $\Phi = V \sin[3\pi \ln(r/a)/\ln(b/a)]$ . Show that within the region,

$$\Phi = V \sinh \left[ \frac{3\pi\phi}{\ln(b/a)} \right] \sin \left[ 3\pi \frac{\ln(r/a)}{\ln(b/a)} \right] / \sinh \left[ \frac{3\pi\alpha}{\ln(b/a)} \right] \quad (a)$$

**5.7.6** The plane  $\phi = 0$  is at potential  $\Phi = V$ , while that at  $\phi = 3\pi/2$  is at zero potential. The system extends to infinity in the  $\pm z$  and  $r$  directions. Determine and sketch  $\Phi$  and  $\mathbf{E}$  in the range  $0 < \phi < 3\pi/2$ .

## 5.8 Examples in Polar Coordinates

**5.8.1\*** Show that  $\Phi$  and  $\mathbf{E}$  as given by (4) and (5), respectively, describe the potential and electric field intensity around a perfectly conducting half-cylinder at  $r = R$  on a perfectly conducting plane at  $x = 0$  with a uniform field  $E_a \mathbf{i}_x$  applied at  $x \rightarrow \infty$ . Show that the maximum field intensity is twice that of the applied field, regardless of the radius of the half-cylinder.

**5.8.2** Coaxial circular cylindrical surfaces bound an annular region of free space where  $b < r < a$ . On the inner surface, where  $r = b$ ,  $\Phi = V_b > 0$ . On the outer surface, where  $r = a$ ,  $\Phi = V_a > 0$ .

- What is  $\Phi$  in the annular region?
- How large must  $V_b$  be to insure that all lines of  $\mathbf{E}$  are outward directed from the inner cylinder?
- What is the net charge per unit length on the inner cylinder under the conditions of (b)?

**5.8.3\*** A device proposed for using the voltage  $v_o$  to measure the angular velocity  $\Omega$  of a shaft is shown in Fig. P5.8.3a. A cylindrical grounded electrode has radius  $R$ . (The resistance  $R_o$  is "small.") Outside and concentric at  $r = a$  is a rotating shell supporting the surface charge density distribution shown in Fig. P5.8.3b.

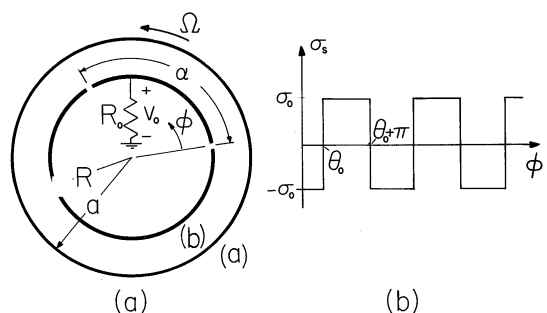


Fig. P5.8.3

- (a) Given  $\theta_o$  and  $\sigma_o$ , show that in regions (a) and (b), respectively, outside and inside the rotating shell,

$$\Phi = \frac{2\sigma_o a}{\pi\epsilon_o} \sum_{\substack{m=1 \\ \text{odd}}}^{\infty} \frac{1}{m^2}. \quad (a)$$

$$\begin{cases} [(a/R)^m - (R/a)^m](R/r)^m \sin m(\phi - \theta_o); & a < r \\ (R/a)^m [(r/R)^m - (R/r)^m] \sin m(\phi - \theta_o); & R < r < a \end{cases}$$

- (b) Show that the charge on the segment of the inner electrode attached to the resistor is

$$q = \sum_{\substack{m=1 \\ \text{odd}}}^{\infty} Q_m [\cos m\theta_o - \cos m(\alpha - \theta_o)]; \quad Q_m \equiv \frac{4w\sigma_o a}{m^2\pi} (R/a)^m \quad (b)$$

where  $w$  is the length in the  $z$  direction.

- (c) Given that  $\theta_o = \Omega t$ , show that the output voltage is related to  $\Omega$  by

$$v_o(t) = \sum_{\substack{m=1 \\ \text{odd}}}^{\infty} Q_m m \Omega R_o [\sin m(\alpha - \Omega t) + \sin m\Omega t] \quad (c)$$

so that its amplitude can be used to measure  $\Omega$ .

- 5.8.4** Complete the steps of Prob. 5.8.3 with the configuration of Fig. P5.8.3 altered so that the rotating shell is inside rather than outside the grounded electrode. Thus, the radius  $a$  of the rotating shell is less than the radius  $R$ , and region (a) is  $a < r < R$ , while region (b) is  $r < a$ .

- 5.8.5\*** A pair of perfectly conducting zero potential electrodes form a wedge, one in the plane  $\phi = 0$  and the other in the plane  $\phi = \alpha$ . They essentially extend to infinity in the  $\pm z$  directions. Closing the region between the electrodes at  $r = R$  is an electrode having potential  $V$ . Show that the potential inside the region bounded by these three surfaces is

$$\Phi = \sum_{\substack{m=1 \\ \text{odd}}}^{\infty} \frac{4V}{m\pi} (r/R)^{m\pi/\alpha} \sin\left(\frac{m\pi\phi}{\alpha}\right) \quad (a)$$

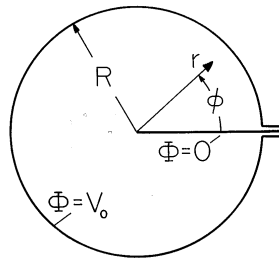


Fig. P5.8.7

- 5.8.6** In a two-dimensional system, the region of interest is bounded in the  $\phi = 0$  plane by a grounded electrode and in the  $\phi = \alpha$  plane by one that has  $\Phi = V$ . The region extends to infinity in the  $r$  direction. At  $r = R$ ,  $\Phi = V$ . Determine  $\Phi$ .
- 5.8.7** Figure P5.8.7 shows a circular cylindrical wall having potential  $V_0$  relative to a grounded fin in the plane  $\phi = 0$  that reaches from the wall to the center. The gaps between the cylinder and the fin are very small.
- Find all solutions in polar coordinates that satisfy the boundary conditions at  $\phi = 0$  and  $\phi = 2\pi$ . Note that you cannot accept solutions for  $\Phi$  of negative powers in  $r$ .
  - Match the boundary condition at  $r = R$ .
  - One of the terms in this solution has an electric field intensity that is infinite at the tip of the fin, where  $r = 0$ . Sketch  $\Phi$  and  $\mathbf{E}$  in the neighborhood of the tip. What is the  $\sigma_s$  on the fin associated with this term as a function of  $r$ ? What is the net charge associated with this term?
  - Sketch the potential and field intensity throughout the region.
- 5.8.8** A two-dimensional system has the same cross-sectional geometry as that shown in Fig. 5.8.6 except that the wall at  $\phi = 0$  has the potential  $v$ . The wall at  $\phi = \phi_0$  is grounded. Determine the interior potential.
- 5.8.9** Use arguments analogous to those used in going from (5.5.22) to (5.5.26) to show the orthogonality (14) of the radial modes  $R_n$  defined by (13). [Note the comment following (14).]

### 5.9 Three Solutions to Laplace's Equation in Spherical Coordinates

- 5.9.1** On the surface of a spherical shell having radius  $r = a$ , the potential is  $\Phi = V \cos \theta$ .
- With no charge density either outside or inside this shell, what is  $\Phi$  for  $r < a$  and for  $r > a$ ?
  - Sketch  $\Phi$  and  $\mathbf{E}$ .



**5.9.2\*** A spherical shell having radius  $a$  supports the surface charge density  $\sigma_o \cos \theta$ .

(a) Show that if this is the only charge in the volume of interest, the potential is

$$\Phi = \frac{\sigma_o a}{3\epsilon_o} \begin{cases} (a/r)^2 \cos \theta & r \geq a \\ (r/a) \cos \theta & r \leq a \end{cases} \quad (a)$$

(b) Show that a plot of  $\Phi$  and  $\mathbf{E}$  appears as shown in Fig. 6.3.1.

**5.9.3\*** A spherical shell having zero potential has radius  $a$ . Inside, the charge density is  $\rho = \rho_o \cos \theta$ . Show that the potential there is

$$\Phi = \frac{a^2 \rho_o}{4\epsilon_o} [(r/a) - (r/a)^2] \cos \theta \quad (a)$$

**5.9.4** The volume of a spherical region is filled with the charge density  $\rho = \rho_o (r/a)^m \cos \theta$ , where  $\rho_o$  and  $m$  are given constants. If the potential  $\Phi = 0$  at  $r = a$ , what is  $\Phi$  for  $r < a$ ?

## 5.10 Three-Dimensional Solutions to Laplace's Equation

**5.10.1\*** In the configuration of Fig. 5.10.2, all surfaces have zero potential except those at  $x = 0$  and  $x = a$ , which have  $\Phi = v$ . Show that

$$\Phi = \sum_{\substack{m=1 \\ \text{odd}}}^{\infty} \sum_{\substack{n=1 \\ \text{odd}}}^{\infty} A_{mn} \sin\left(\frac{m\pi y}{b}\right) \sin\left(\frac{n\pi z}{w}\right) \cosh k_{mn} \left(x - \frac{a}{2}\right) \quad (a)$$

and

$$A_{mn} = \frac{16v}{mn\pi^2} / \cosh \frac{k_{mn}a}{2} \quad (b)$$

**5.10.2** In the configuration of Fig. 5.10.2, all surfaces have zero potential. In the plane  $y = a/2$ , there is the surface charge density  $\sigma_s = \sigma_o \sin(\pi x/a) \sin(\pi z/w)$ . Find the potentials  $\Phi^a$  and  $\Phi^b$  above and below this surface, respectively.

**5.10.3** The configuration is the same as shown in Fig. 5.10.2 except that all of the walls are at zero potential and the volume is filled by the uniform charge density  $\rho = \rho_o$ . Write four essentially different expressions for the potential distribution.